
Astronomy 233 Winter 2009
Physical Cosmology
Weeks 7 & 8
Cosmic Background, Phase Transitions, Defects, & Inflation
Joel Primack
University of California, Santa Cruz

CMB, Phase Transitions, Cosmic Defects, and Inflation

Weeks 7 and 8

Outline

Cosmic Microwave Background
WMAP 5-year Data and Papers Released
Grand Unification of Forces
Phase Transitions in the Early Universe
Topological Defects: Strings, Monopoles
Cosmic Inflation

Cosmic Microwave Background

Early History

Although Penzias and Wilson discovered the CMB in 1965, Weinberg (p. 104) points out that Adams and McKellar had shown that the rotational spectra of cyanogen (CN) molecules observed in 1941 suggested that the background temperature is about 3K.

The COBE FIRAS measurements showed that the spectrum is that of thermal radiation with T = 2.73K.

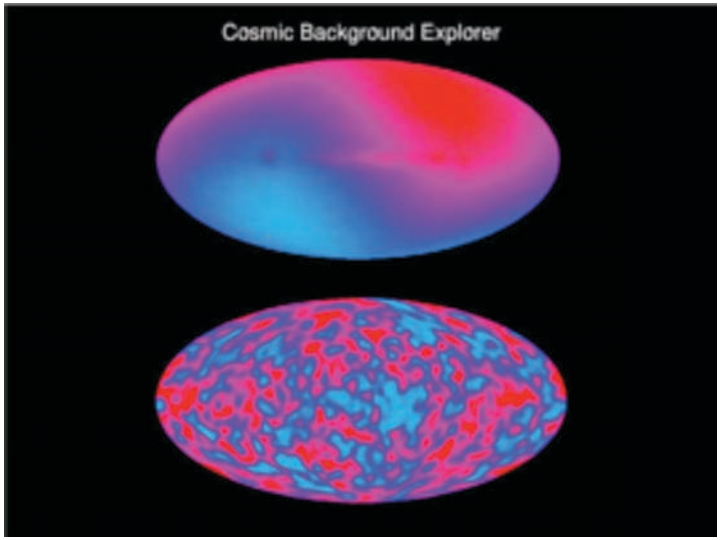

The CMB dipole anisotropy was discovered by Paul Henry (1971) and Edward Conklin (1972), and confirmed by Conklin and Wilkinson (1977) and Smoot, Gorenstein, and Muller (1977) -- see http://www.astro.ucla.edu/~wright/CMB-dipole-history.html

The upper panel of the figure shows the CMB dipole anisotropy in the COBE data. It is usually subtracted when the temperature anisotropy map is displayed (lower panel).

CMB Temperature Anisotropy

Sachs & Wolfe (1967, ApJ, 147, 73) showed that on large angular scales the temperature anisotropy is $\Delta T/T = \varphi/3c^2$. White & Hu give a pedagogical derivation in http://background.uchicago.edu/~whu/Papers/sw.pdf

PERTURBATIONS OF A COSMOLOGICAL MODEL AND ANGULAR VARIATIONS OF THE MICROWAVE BACKGROUND

R. K. SACHS AND A. M. WOLFE
Relativity Center, The University of Texas, Austin, Texas
Received May 13, 1966

ABSTRACT

We consider general-relativistic, spatially homogeneous, and isotropic $k = 0$ cosmological models with either pressure zero or pressure one-third the energy density. The equations for general linearized perturbations away from these models are explicitly integrated to obtain density fluctuations, rotational perturbations, and gravitational waves. The equations for light rays in the perturbed models are integrated. The models are used to estimate the anisotropy of the microwave radiation, assuming this radiation is cosmological It is estimated that density fluctuations now of order 10 per cent with characteristic lengths now of order 1000 Mpc would cause anisotropies of order 1 per cent in the observed microwave temperature due to the gravitational redshift and other general-relativistic effects. The $p = 0$ models are compared in detail with corresponding Newtonian models The perturbed Newtonian models do not contain gravitational waves, but the density perturbations and rotational perturbations are surprisingly similar.

This was first convincingly seen by the COBE DMR experiment, reported by George Smoot on April 27, 1992. Their result $\Delta T/T = 10^{-5}$ had been predicted by the CDM model (Blumenthal, Faber, Primack, & Rees 1984). The search then began for smaller-angular-scale CMB anisotropies.

CMB

Shown at DM2000:

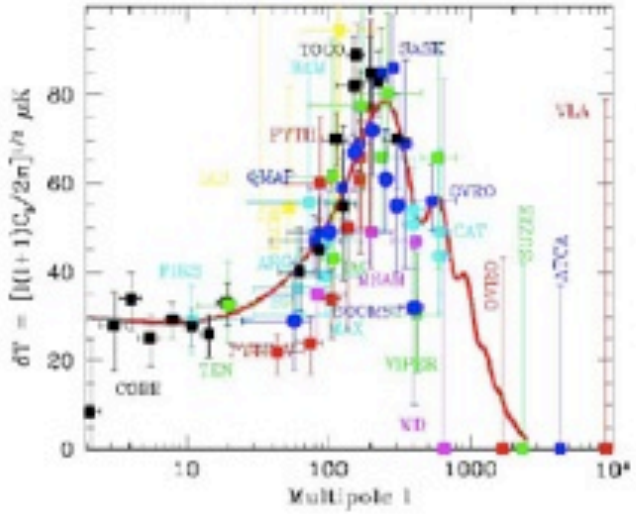

Max Tegmark

CMB

Shown at DM2002:

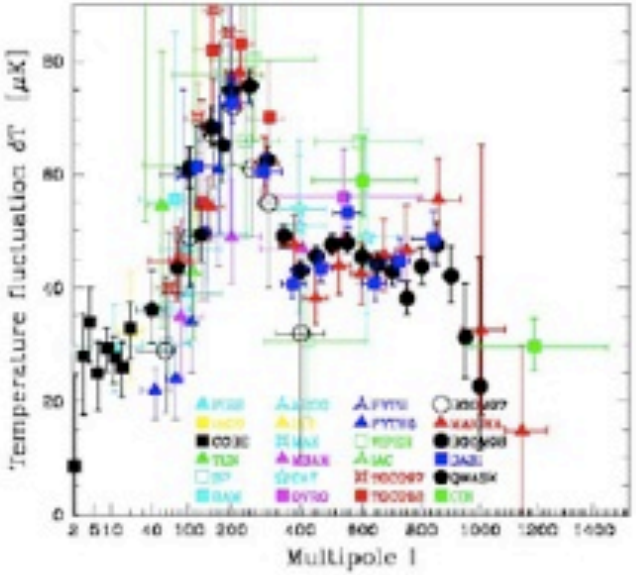

CMB

Shown at DM2004:

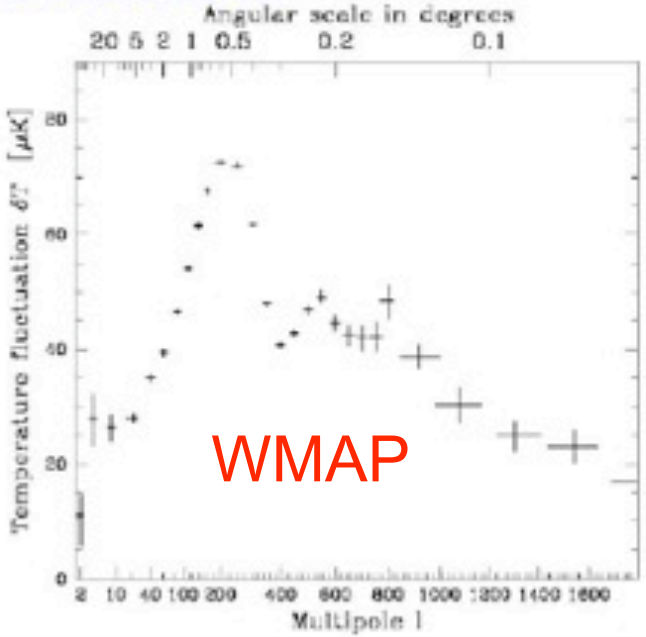

Shown at DM2006:

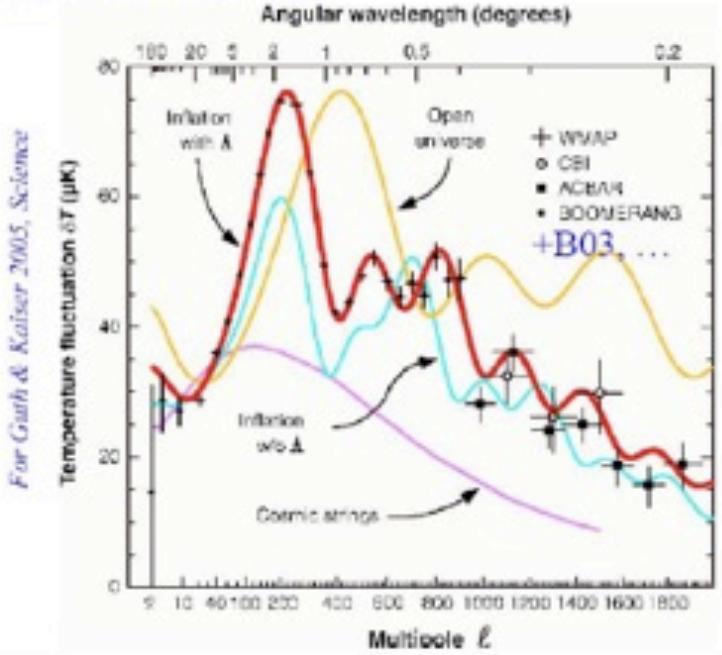

THE COSMIC SYMPHONY

By Wayne Hu and Martin White

New observations of the cosmic microwave background radiation show that the early universe resounded with harmonious oscillations

Scientific American February 2004

THE POWER SPECTRUM

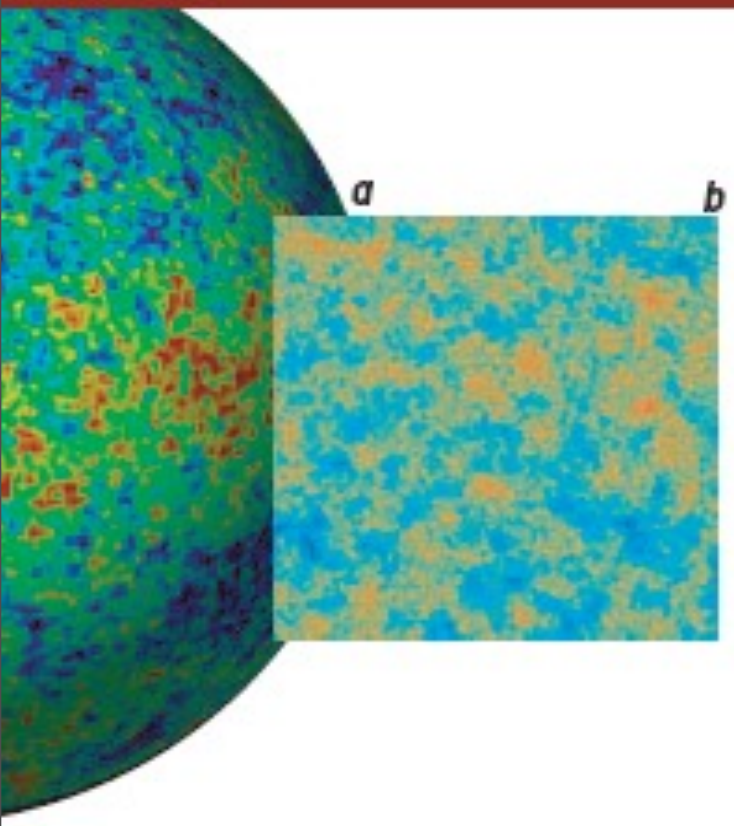

OBSERVATIONS OF THE CMB provide a map of temperature variations across the whole sky (*a*). When researchers analyze portions of that map (*b*), they use band filters to show how the temperature of the radiation varies at different scales. The variations are barely noticeable at large scales corresponding to regions that stretch about 30 degrees across the sky (*c*) and at small scales corresponding to regions about a tenth of a degree across (*e*). But the temperature differences are quite distinct for regions about one degree across (*d*). This first peak in the power spectrum (*graph at bottom*) reveals the compressions and rarefactions caused by the fundamental wave of the early universe; the subsequent peaks show the effects of the overtones.

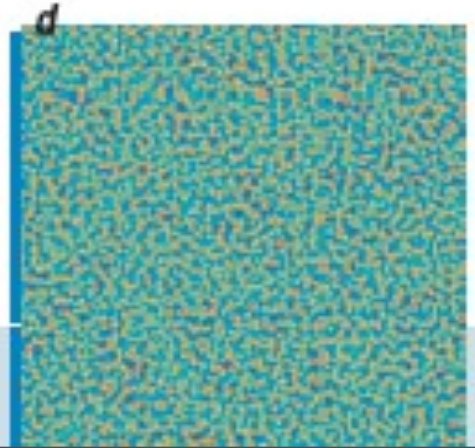

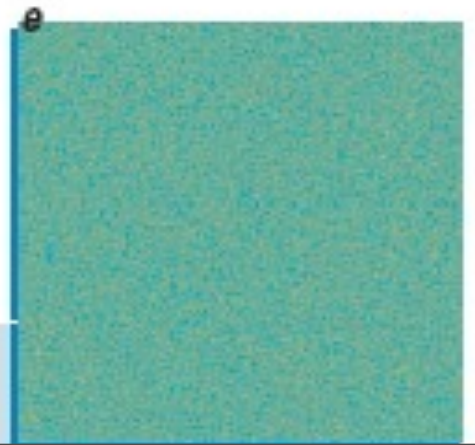

Angular Thermal Variations

30° barely visible

1° prominent

0.1° barely visible

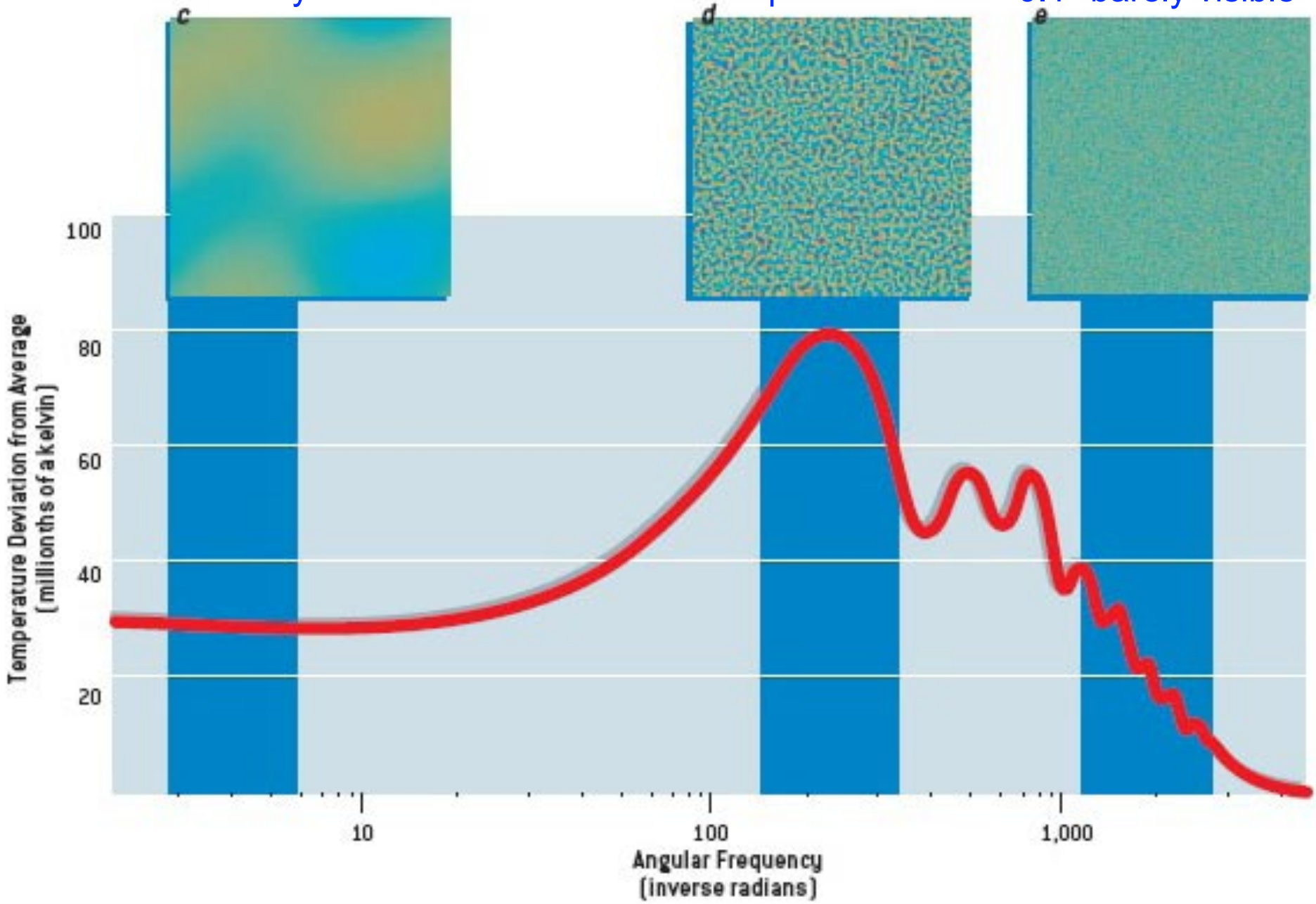

GRAVITATIONAL MODULATION

INFLUENCE OF DARK MATTER modulates the acoustic signals in the CMB. After inflation, denser regions of dark matter that have the same scale as the fundamental wave (*represented as troughs in this potential-energy diagram*) pull in baryons and photons by gravitational attraction. (The troughs are shown in red because gravity also reduces the temperature of any escaping photons.) By the time of recombination, about 380,000 years later, gravity and sonic motion have worked together to raise the radiation temperature in the troughs (*blue*) and lower the temperature at the peaks (*red*).

FIRST PEAK

Gravity and sonic motion work together

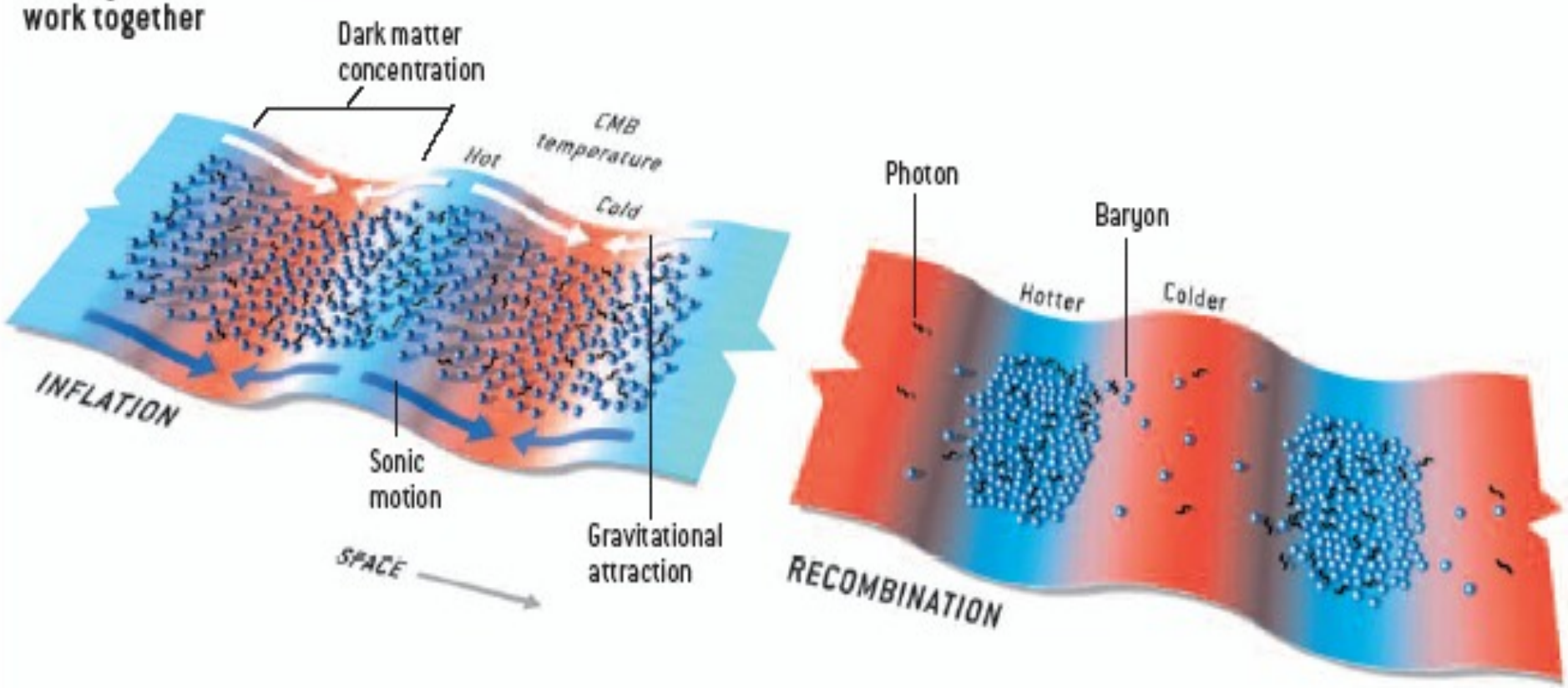

AT SMALLER SCALES, gravity and acoustic pressure sometimes end up at odds. Dark matter clumps corresponding to a second-peak wave maximize radiation temperature in the troughs long before recombination. After this midpoint, gas pressure pushes baryons and photons out of the troughs (*blue arrows*) while gravity tries to pull them back in (*white arrows*). This tug-of-war decreases the temperature differences, which explains why the second peak in the power spectrum is lower than the first.

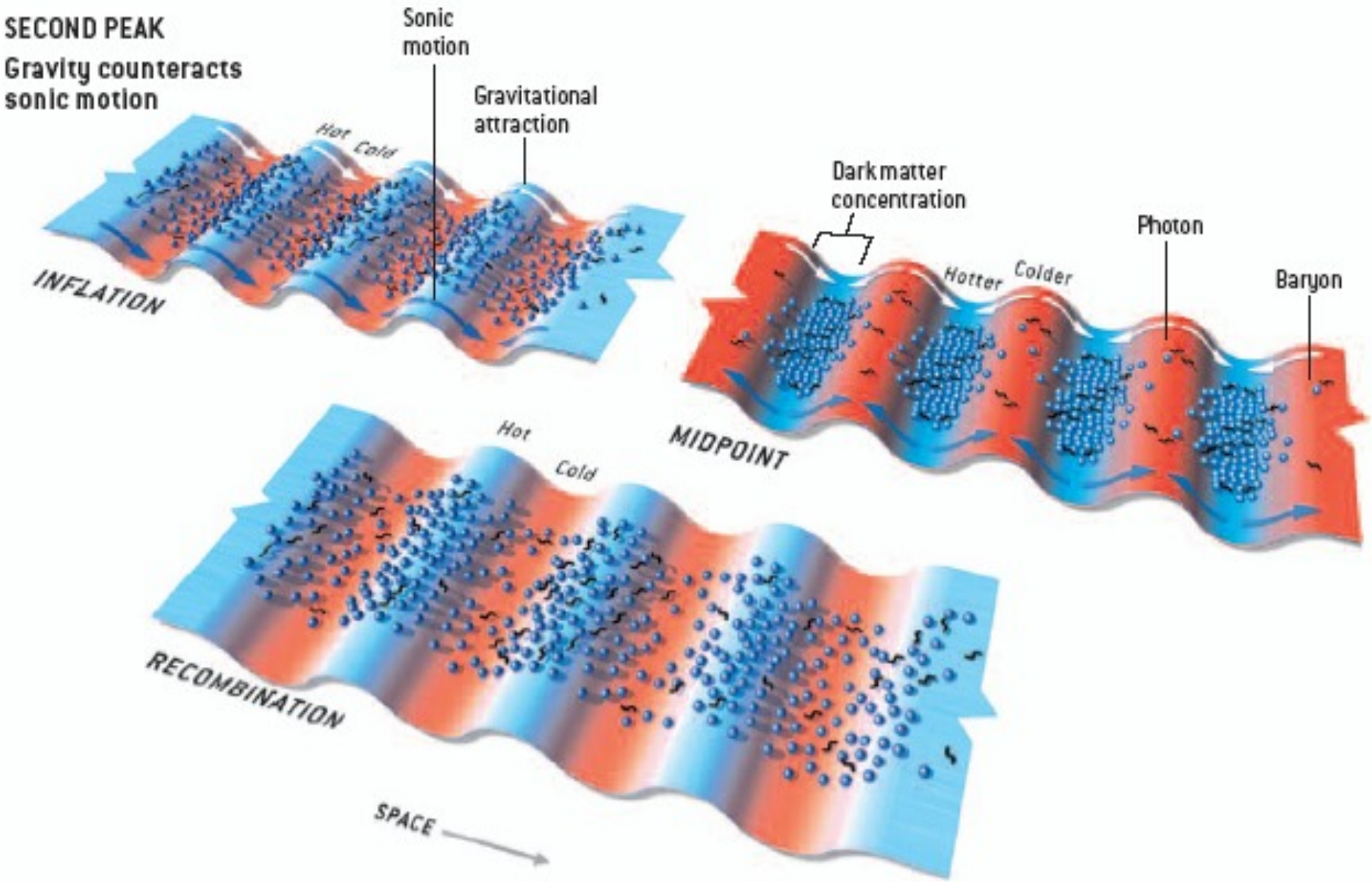

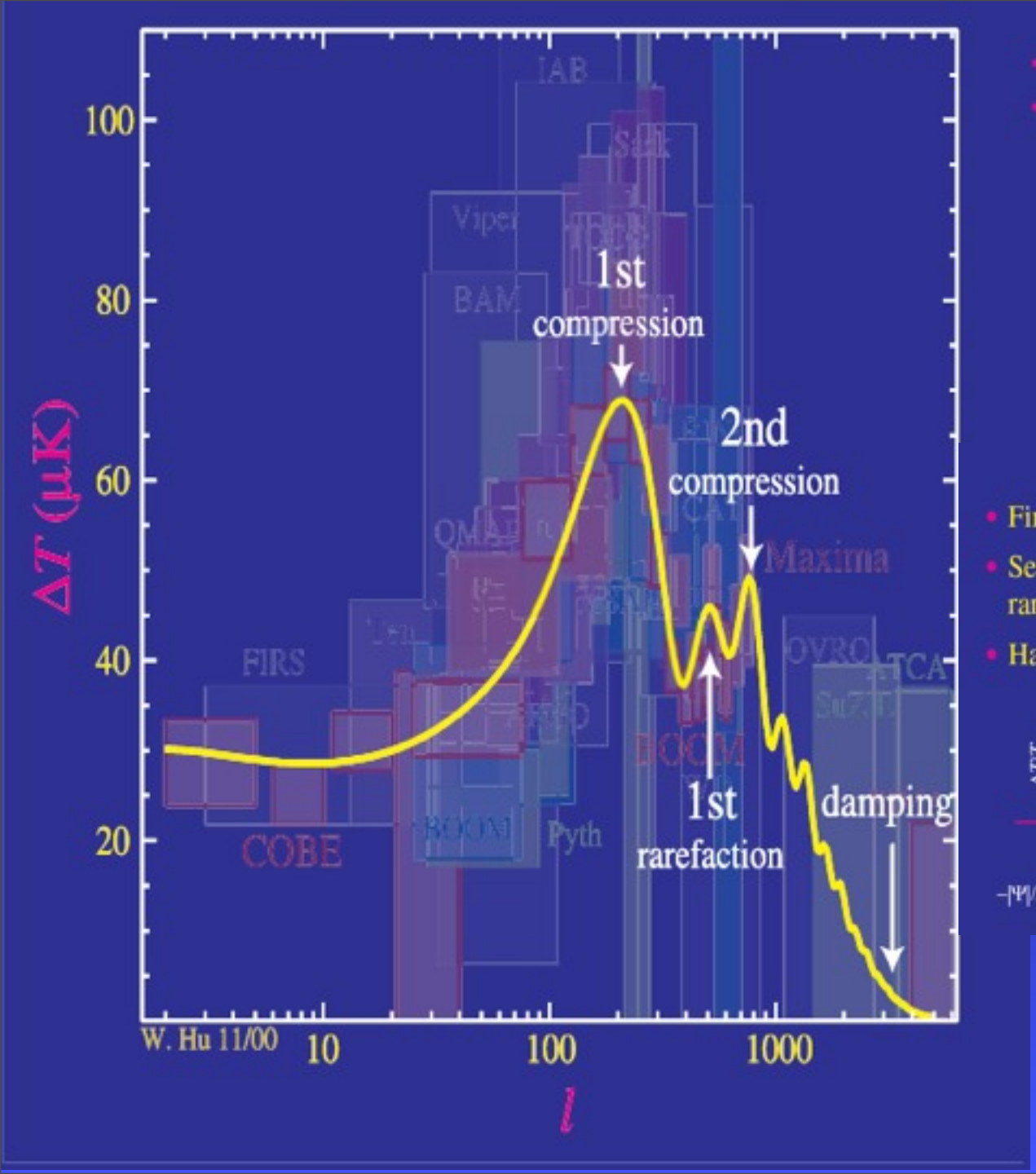

Gravitational Ringing

- Potential wells = inflationary seeds of structure
- Fluid falls into wells, pressure resists: acoustic oscillations

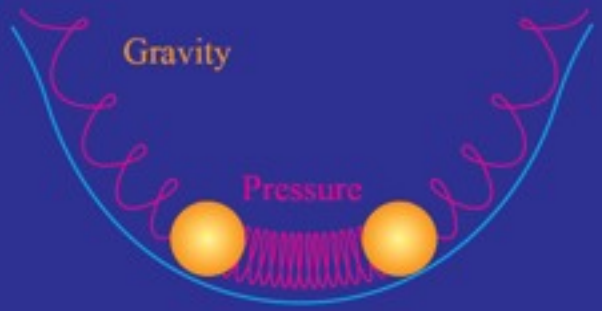

Extrema=Peaks

- First peak = mode that just compresses
- Second peak = mode that compresses then rarefies: twice the wavenumber
- Harmonic peaks: 1:2:3 in wavenumber

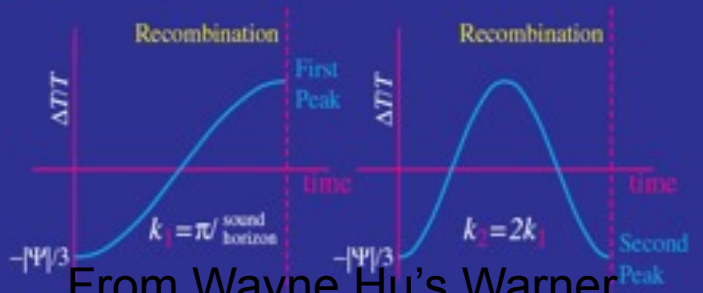

From Wayne Hu's Warner Prize Lecture, AAS meeting Jan 2001:
http://background.uchicago.edu/~whu/Presentations/warnerprint.pdf

Sound Spectrum

- Spectrum of sound shows harmonics at integer ratios of the fundamental
- Other models that generate structure causally at intermediate times would not have these harmonics

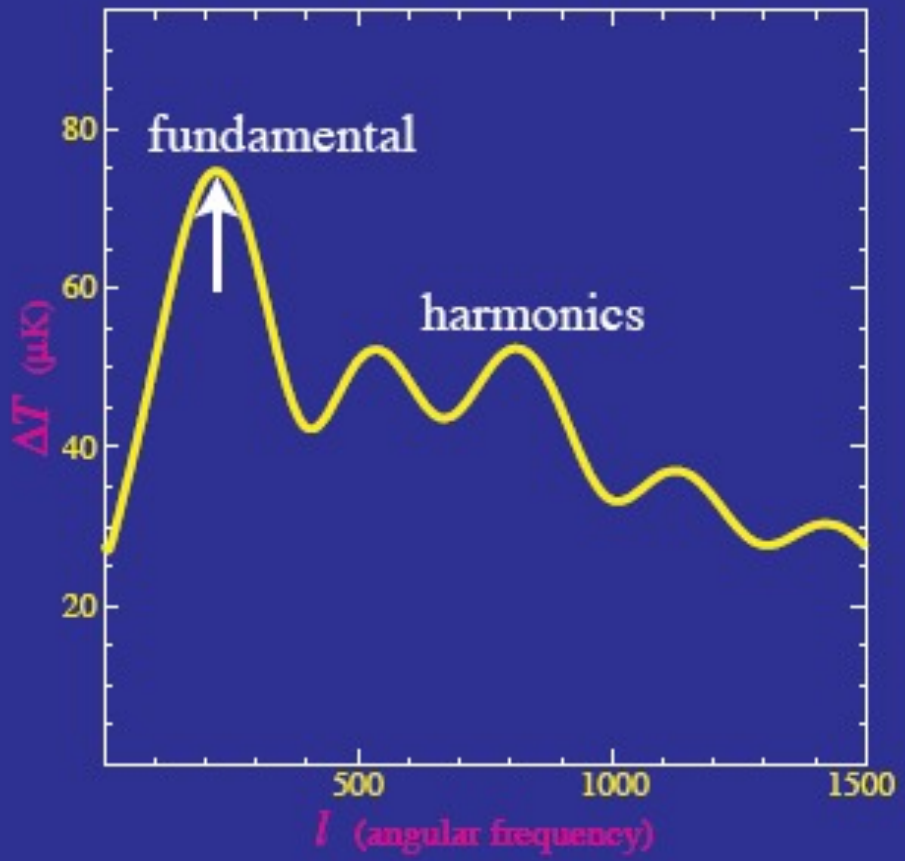

Dark Matter

- A third peak comparable to second peak indicates a dark matter density ~5x that of ordinary matter
- Dark matter ~25% of the critical density

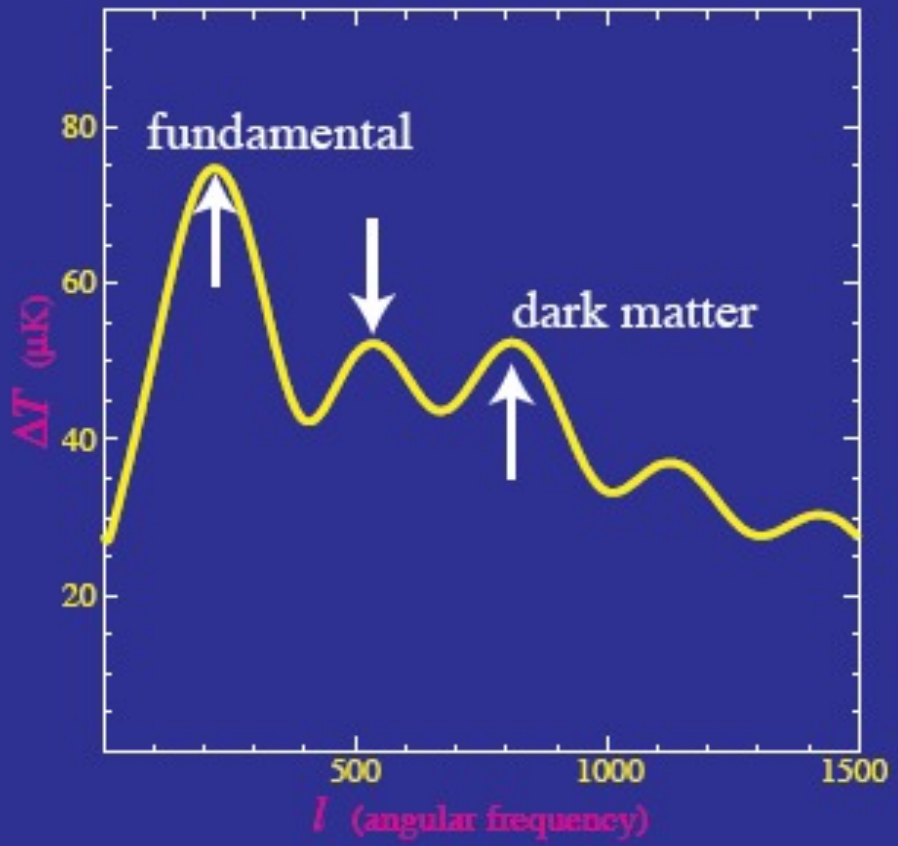

Predictive Power

- Model predicts the precise form of the damping of sound waves: observed ✔
- Model predicts that associated with the damping, the CMB becomes polarized: observed ✔
- Model predicts that temperature fluctuations correlated with local structure due to the dark energy: observed ✔

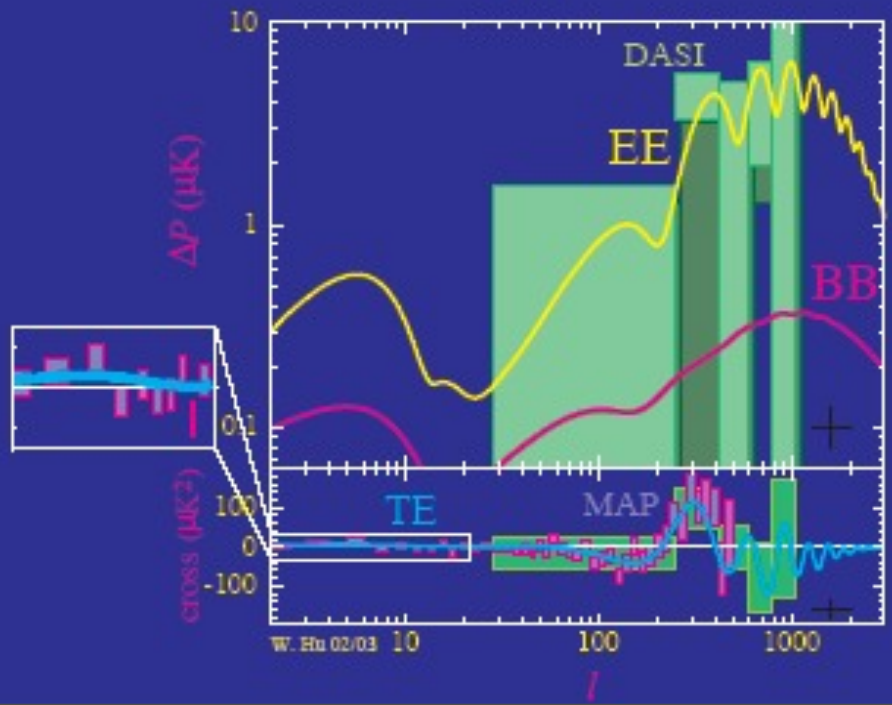

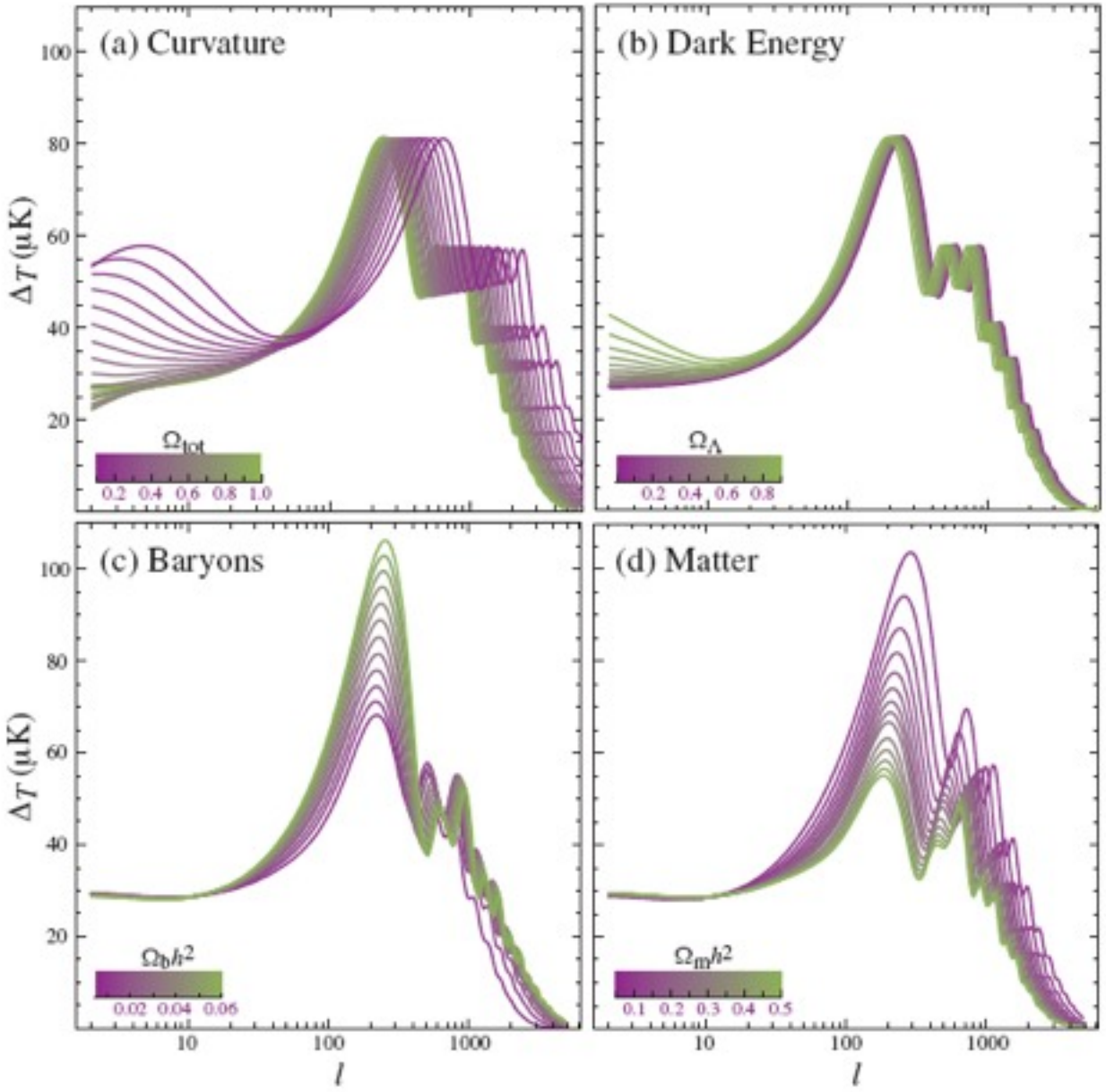

Plate 4: Sensitivity of the acoustic temperature spectrum to four fundamental cosmological parameters (a) the curvature as quantified by Ω_{tot} (b) the dark energy as quantified by the cosmological constant Ω_Λ ($w_\Lambda = -1$) (c) the physical baryon density $\Omega_b h^2$ (d) the physical matter density $\Omega_m h^2$, all varied around a fiducial model of $\Omega_{tot} = 1$, $\Omega_\Lambda = 0.65$, $\Omega_b h^2 = 0.02$, $\Omega_m h^2 = 0.147$, $n = 1$, $z_{ri} = 0$, $E_i = 0$.

Annu. Rev. Astron. and Astrophys. 2002
Cosmic Microwave Background Anisotropies by **Wayne Hu** and **Scott Dodelson**

For animation of the effects of changes in cosmological parameters on the CMB angular power spectrum and the matter power spectrum, plus links to many CMB websites, see Max Tegmark's and Wayne Hu's websites:

http://space.mit.edu/home/tegmark/

http://background.uchicago.edu/~whu/physics/physics.html

WMAP 5-year data and papers are at http://lambda.gsfc.nasa.gov/

G. Hinshaw et al. ApJS, 180, 225 (2009)

Five-Year Wilkinson Microwave Anisotropy Probe (WMAP[1]) Observations: Data Processing, Sky Maps, & Basic Results

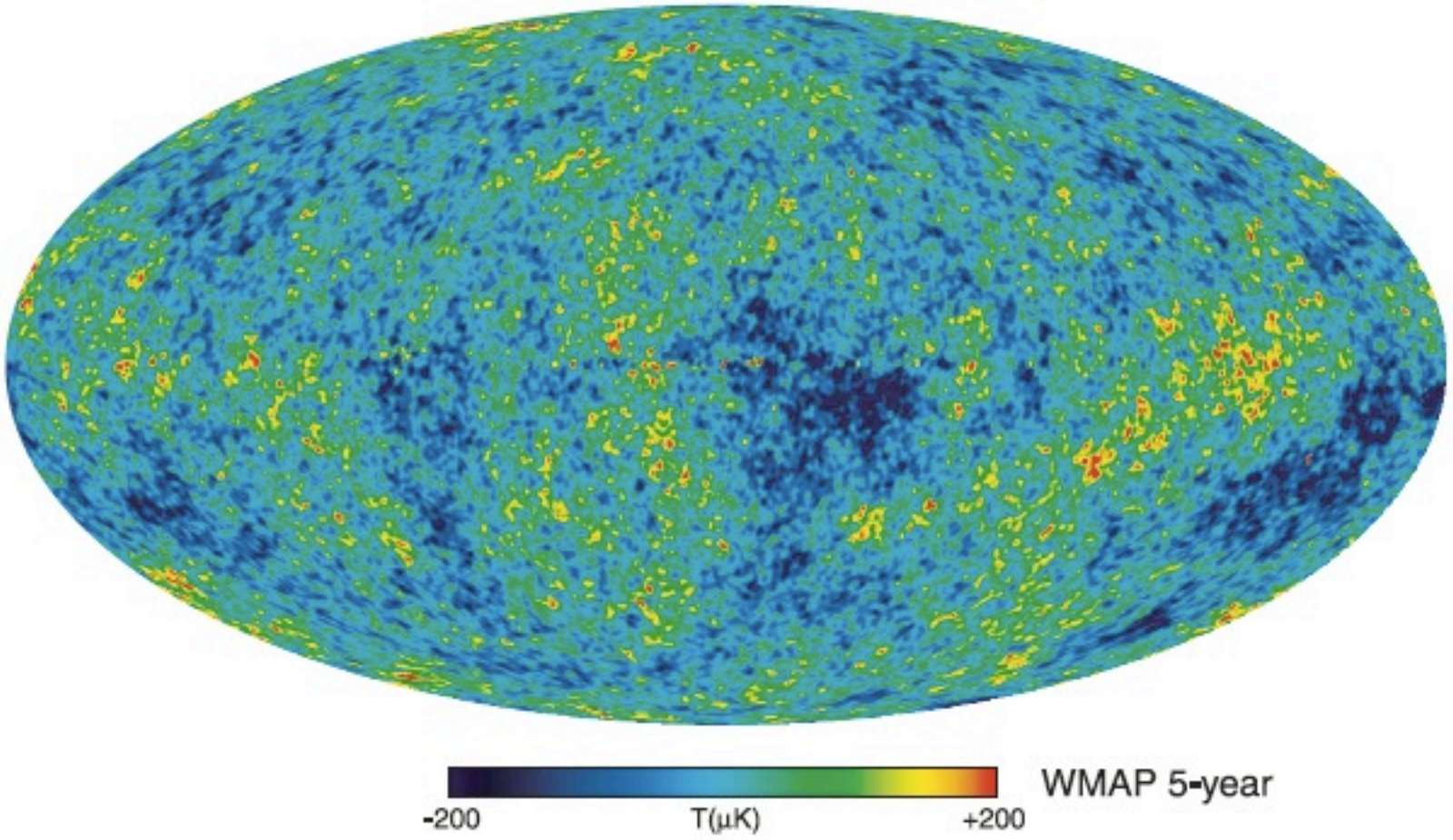

Fig. 12. The foreground-reduced Internal Linear Combination (ILC) map based on the 5 year WMAP data.

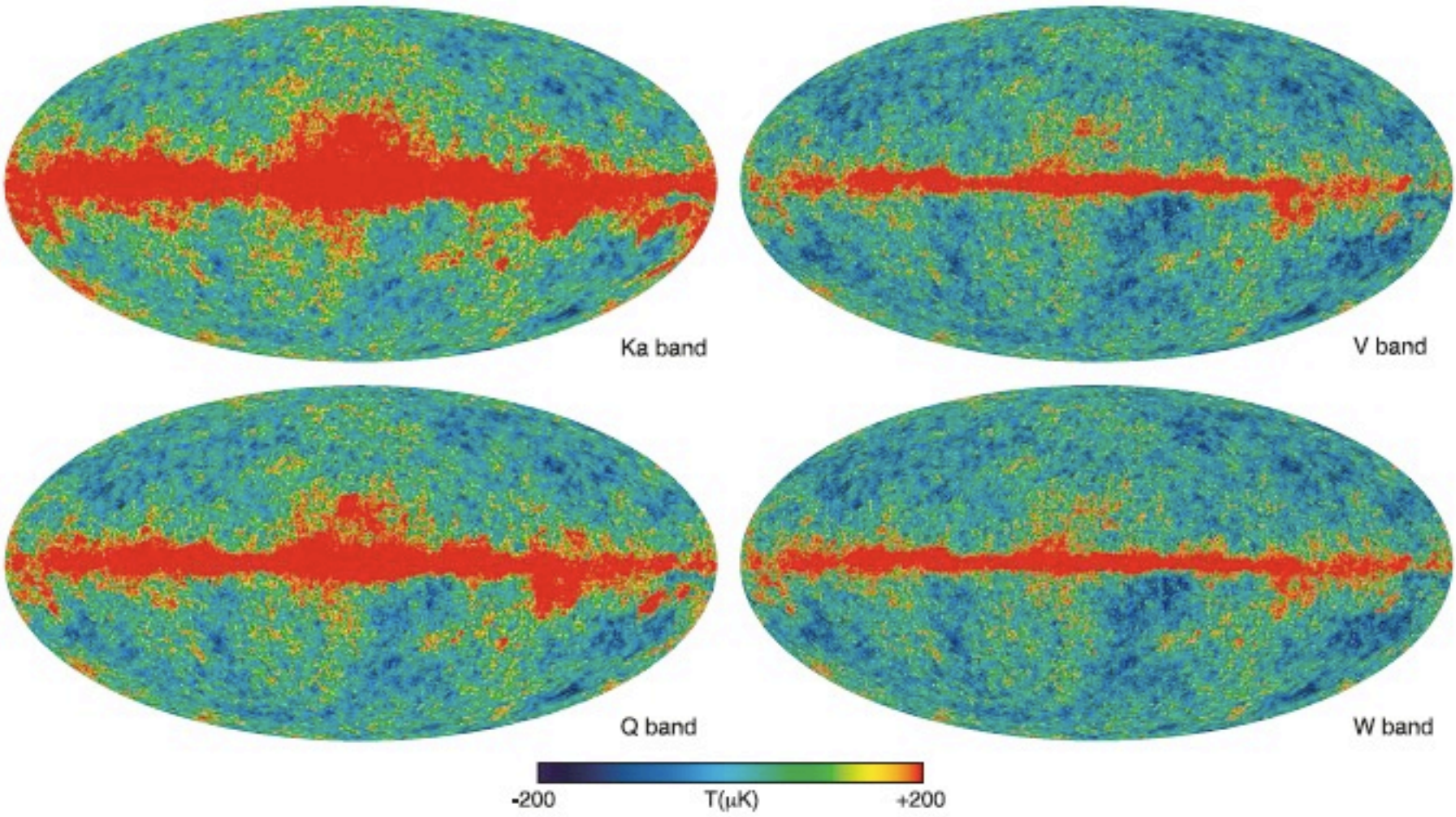

Fig. 1.— Five-year temperature sky maps in Galactic coordinates smoothed with a 0.2° Gaussian beam, shown in Mollweide projection. ~~*top*: K band (23 GHz)~~, *middle-left*: Ka band (33 GHz), *bottom-left*: Q band (41 GHz), *middle-right*: V band (61 GHz), *bottom-right*: W band (94 GHz). Note: only V and W bands are used for cosmological analysis.

G. Hinshaw et al.ApJS, 180, 225 (2009)

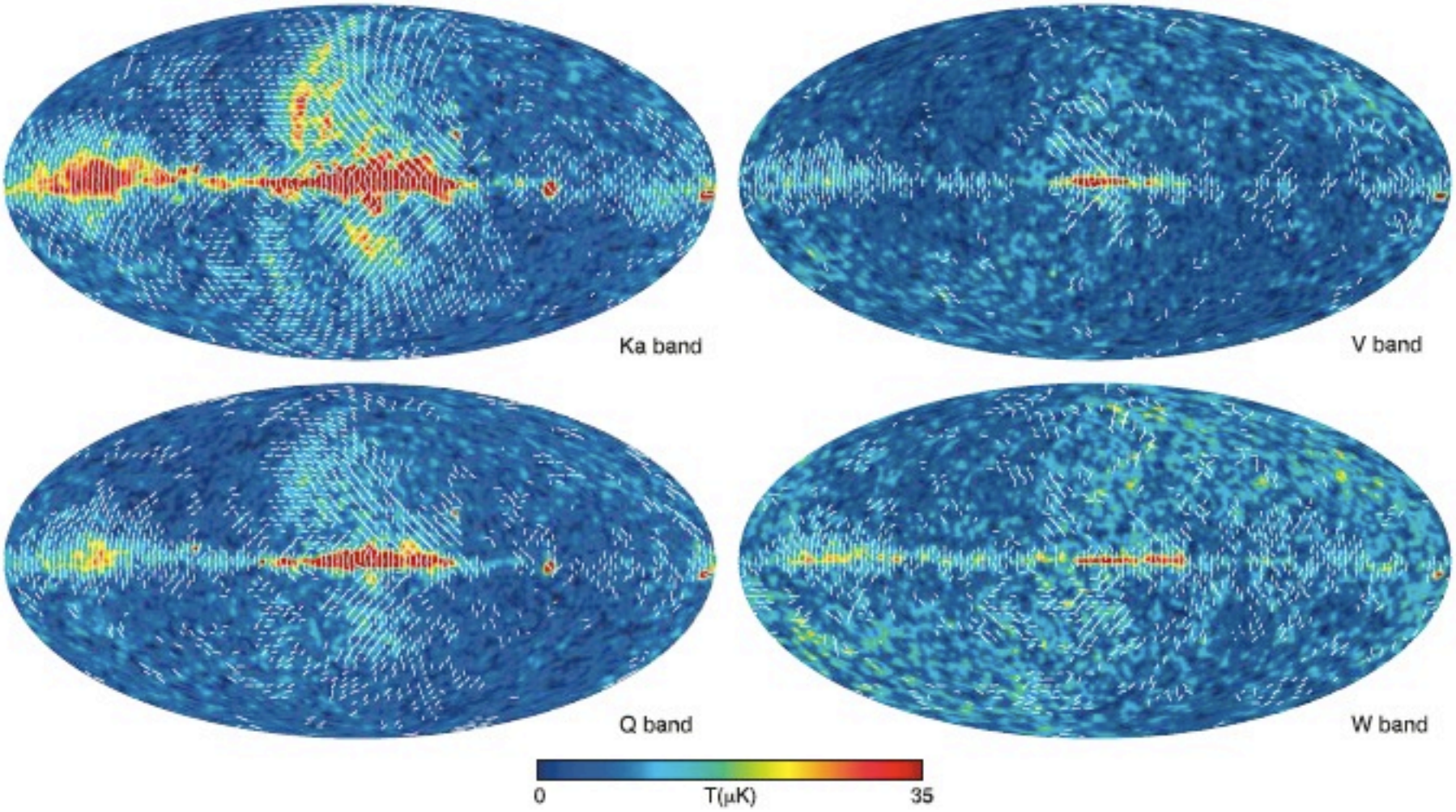

Fig. 4.— Five-year polarization sky maps in Galactic coordinates smoothed to an effective Gaussian beam of 2.0°, shown in Mollweide projection. The color scale indicates polarized intensity, $P = \sqrt{Q^2 + U^2}$, and the line segments indicate polarization direction in pixels whose signal-to-noise exceeds 1. *top*: K band (23 GHz), *middle-left*: Ka band (33 GHz), *bottom-left*: Q band (41 GHz), *middle-right*: V band (61 GHz), *bottom-right*: W band (94 GHz). G. Hinshaw et al.ApJS, 180, 225 (2009)

Fig. 13. The temperature (TT) and temperature-polarization correlation (TE) power spectra based on the 5 year WMAP data. The addition of 2 years of data provide more sensitive measurements of the third peak in TT and the high-l TE spectrum, especially the second trough.

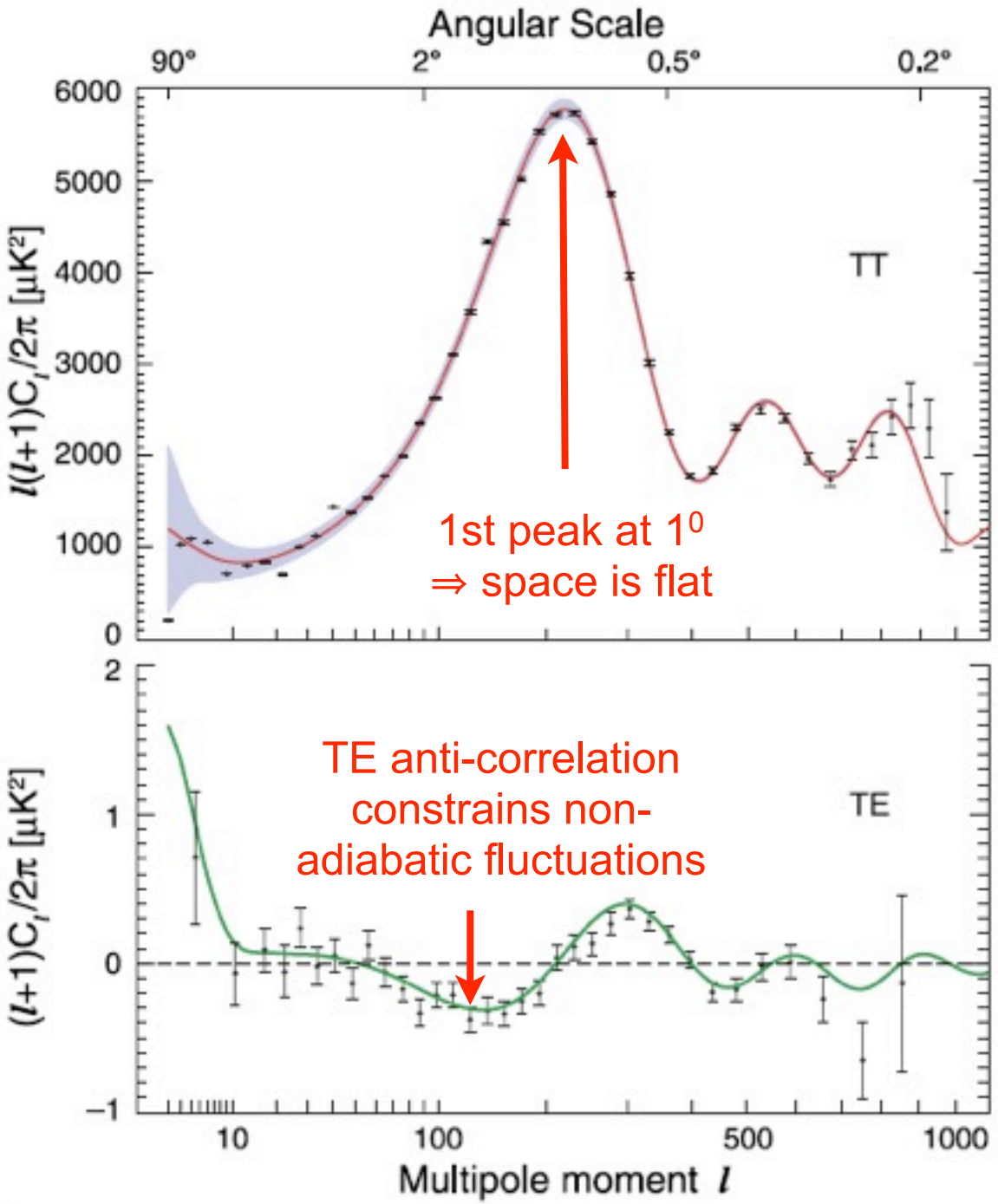

G. Hinshaw et al.
ApJS, 180, 225 (2009)

Five-Year Wilkinson Microwave Anisotropy Probe (WMAP[1]) Observations: Data Processing, Sky Maps, & Basic Results

The cosmological implications of the 5 year *WMAP* data are discussed in detail in Dunkley et al. (2008) and Komatsu et al. (2008). The now-standard cosmological model: a flat universe dominated by vacuum energy and dark matter, seeded by nearly scale-invariant, adiabatic, Gaussian random-phase fluctuations, continues to fit the 5 year data. *WMAP* has now determined the key parameters of this model to high precision; a summary of the 5 year parameter results is given in Table 6. The most notable improvements are the measurements of the dark matter density, $\Omega_c h^2$, and the amplitude of matter fluctuations today, σ_8. The former is determined with 6% uncertainty using *WMAP* data only (Dunkley et al. 2008), and with 3% uncertainty when *WMAP* data is combined with BAO and SNe constraints (Komatsu et al. 2008). The latter is measured to 5% with *WMAP* data, and to 3% when combined with other data. The redshift of reionization is $z_{\rm reion} = 11.0 \pm 1.4$, if the universe were reionized instantaneously. The 2 σ lower limit is $z_{\rm reion} > 8.2$, and instantaneous reionization at $z_{\rm reion} = 6$ is rejected at 3.5 σ. The *WMAP* data continues to favor models with a tilted primordial spectrum, $n_s = 0.963^{+0.014}_{-0.015}$. Dunkley et al. (2008) discuss how the ΛCDM model continues to fit a host of other astronomical data as well.

Moving beyond the standard ΛCDM model, when *WMAP* data is combined with BAO and SNe observations (Komatsu et al. 2008), we find no evidence for running in the spectral index of scalar fluctuations, $dn_s/d\ln k = -0.032^{+0.021}_{-0.020}$ (68% CL). The new limit on the tensor-to-scalar ratio is $r < 0.20$ (95% CL), and we obtain tight, simultaneous limits on the (constant) dark energy equation of state and the spatial curvature of the universe: $-0.11 < 1 + w < 0.14$ (95% CL) and $-0.0175 < \Omega_k < 0.0085$ (95% CL). The angular power spectrum now exhibits the signature of the cosmic neutrino background: the number of relativistic degrees of freedom, expressed in units of the effective number of neutrino species, is found to be $N_{\rm eff} = 4.4 \pm 1.5$ (68% CL), consistent with the standard value of 3.04. Models with $N_{\rm eff} = 0$ are disfavored at >99.5% confidence. A summary of the key cosmological parameter values is given in Table 6, where we provide estimates using *WMAP* data alone and *WMAP* data combined with BAO and SNe observations. A complete tabulation of all parameter values for each model and dataset combination we studied is available on LAMBDA.

Description	Symbol	*WMAP*-only	*WMAP*+BAO+SN
Parameters for Standard ΛCDM Model [a]			
Age of universe	t_0	13.69 ± 0.13 Gyr	13.73 ± 0.12 Gyr
Hubble constant	H_0	$71.9^{+2.6}_{-2.7}$ km/s/Mpc	70.1 ± 1.3 km/s/Mpc
Baryon density	Ω_b	0.0441 ± 0.0030	0.0462 ± 0.0015
Physical baryon density	$\Omega_b h^2$	0.02273 ± 0.00062	0.02265 ± 0.00059
Dark matter density	Ω_c	0.214 ± 0.027	0.233 ± 0.013
Physical dark matter density	$\Omega_c h^2$	0.1099 ± 0.0062	0.1143 ± 0.0034
Dark energy density	Ω_Λ	0.742 ± 0.030	0.721 ± 0.015
Curvature fluctuation amplitude, $k_0 = 0.002$ Mpc^{-1} [b]	$\Delta^2_{\mathcal{R}}$	$(2.41 \pm 0.11) \times 10^{-9}$	$(2.457^{+0.092}_{-0.093}) \times 10^{-9}$
Fluctuation amplitude at $8h^{-1}$ Mpc	σ_8	0.796 ± 0.036	0.817 ± 0.026
$l(l+1)C^{TT}_{220}/2\pi$	C_{220}	5756 ± 42 μK^2	5748 ± 41 μK^2
Scalar spectral index	n_s	$0.963^{+0.014}_{-0.015}$	$0.960^{+0.014}_{-0.013}$
Redshift of matter-radiation equality	$z_{\rm eq}$	3176^{+151}_{-150}	3280^{+88}_{-89}
Angular diameter distance to matter-radiation eq.[c]	$d_A(z_{\rm eq})$	14279^{+186}_{-189} Mpc	14172^{+141}_{-139} Mpc
Redshift of decoupling	z_*	1090.51 ± 0.95	$1091.00^{+0.72}_{-0.73}$
Age at decoupling	t_*	380081^{+5843}_{-5841} yr	375938^{+3148}_{-3115} yr
Angular diameter distance to decoupling [c,d]	$d_A(z_*)$	14115^{+188}_{-191} Mpc	14006^{+142}_{-141} Mpc
Sound horizon at decoupling [d]	$r_s(z_*)$	146.8 ± 1.8 Mpc	145.6 ± 1.2 Mpc
Acoustic scale at decoupling [d]	$l_A(z_*)$	$302.08^{+0.83}_{-0.84}$	$302.11^{+0.84}_{-0.82}$
Reionization optical depth	τ	0.087 ± 0.017	0.084 ± 0.016
Redshift of reionization	$z_{\rm reion}$	11.0 ± 1.4	10.8 ± 1.4
Age at reionization	$t_{\rm reion}$	427^{+88}_{-65} Myr	432^{+90}_{-67} Myr

Parameters for Extended Models [e]

Total density [f]	$\Omega_{\rm tot}$	$1.099^{+0.100}_{-0.085}$	1.0052 ± 0.0064
Equation of state [g]	w	$-1.06^{+0.41}_{-0.42}$	$-0.972^{+0.061}_{-0.060}$
Tensor to scalar ratio, $k_0 = 0.002$ Mpc^{-1} [b,h]	r	< 0.43 (95% CL)	< 0.20 (95% CL)
Running of spectral index, $k_0 = 0.002$ Mpc^{-1} [b,i]	$dn_s/d\ln k$	-0.037 ± 0.028	$-0.032^{+0.021}_{-0.020}$
Neutrino density [j]	$\Omega_\nu h^2$	< 0.014 (95% CL)	< 0.0065 (95% CL)
Neutrino mass [j]	$\sum m_\nu$	< 1.3 eV (95% CL)	< 0.61 eV (95% CL)
Number of light neutrino families [k]	$N_{\rm eff}$	> 2.3 (95% CL)	4.4 ± 1.5

[a]The parameters reported in the first section assume the 6 parameter ΛCDM model, first using *WMAP* data only (Dunkley et al. 2008), then using *WMAP*+BAO+SN data (Komatsu et al. 2008).

[b]$k = 0.002$ Mpc$^{-1} \longleftrightarrow l_{\rm eff} \approx 30$.

[c]Comoving angular diameter distance.

[d]$l_A(z_*) \equiv \pi d_A(z_*) r_s(z_*)^{-1}$.

[e]The parameters reported in the second section place limits on deviations from the ΛCDM model, first using *WMAP* data only (Dunkley et al. 2008), then using *WMAP*+BAO+SN data (Komatsu et al. 2008). A complete listing of all parameter values and uncertainties for each of the extended models studied is available on LAMBDA.

[f]Allows non-zero curvature, $\Omega_k \neq 0$.

[g]Allows $w \neq -1$, but assumes w is constant.

[h]Allows tensors modes but no running in scalar spectral index.

[i]Allows running in scalar spectral index but no tensor modes.

[j]Allows a massive neutrino component, $\Omega_\nu \neq 0$.

[k]Allows $N_{\rm eff}$ number of relativistic species. The last column adds the HST prior to the other data sets.

Komatsu et al.

ApJS, 180, 330 (2009)

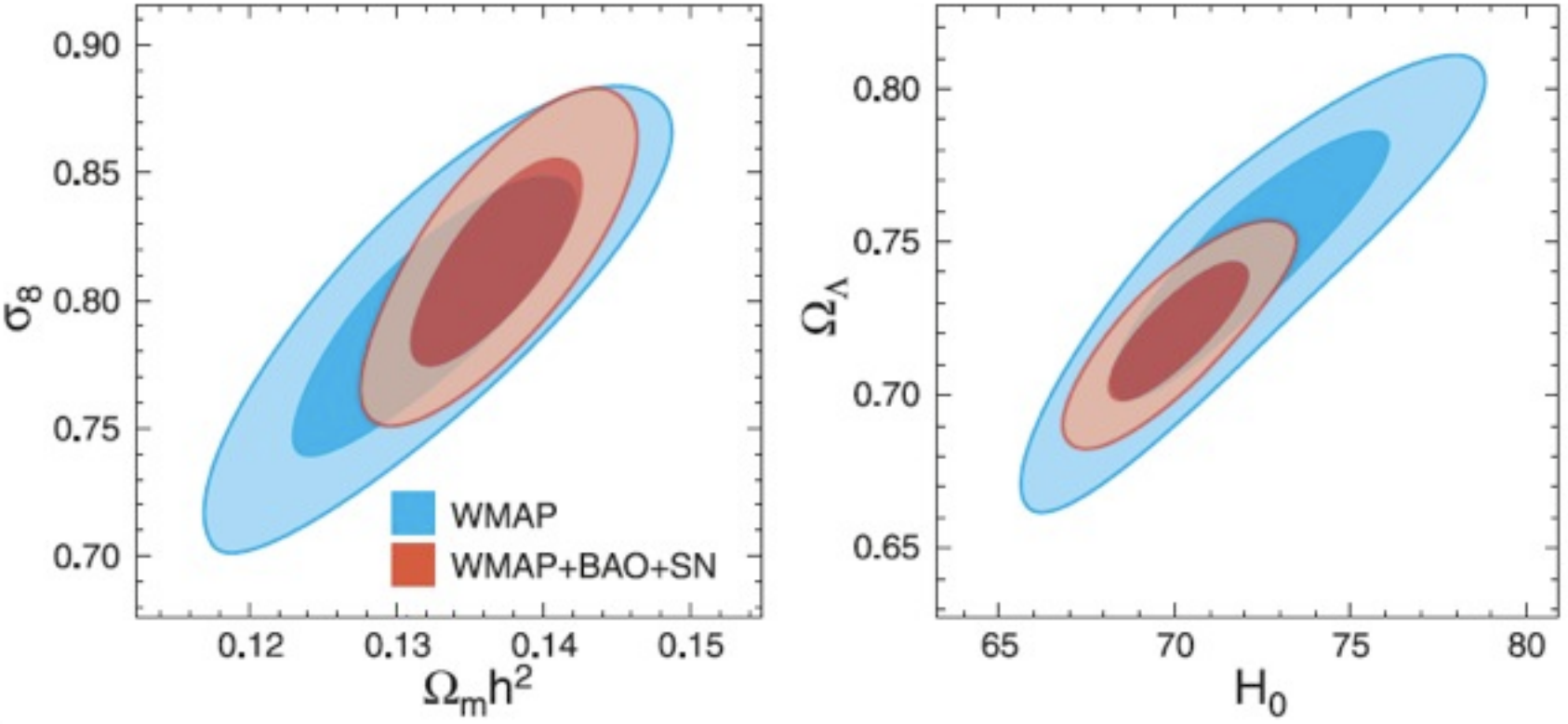

7. CONCLUSION

With 5 years of integration, the *WMAP* temperature and polarization data have improved significantly. An improved determination of the third acoustic peak has enabled us to reduce the uncertainty in the amplitude of matter fluctuation, parametrized by σ_8, by a factor of 1.4 from the *WMAP* 3-year result. The E-mode polarization is now detected at 5 standard deviations (c.f., 3.0 standard deviations for the 3-year data; Page et al. 2007), which rules out an instantaneous reionization at $z_{\rm reion} = 6$ at the 3.5σ level. Overall, the *WMAP* 5-year data continue to support the simplest, 6-parameter ΛCDM model (Dunkley et al. 2008).

Komatsu et al. *WMAP* 5-year Cosmological Interpretation

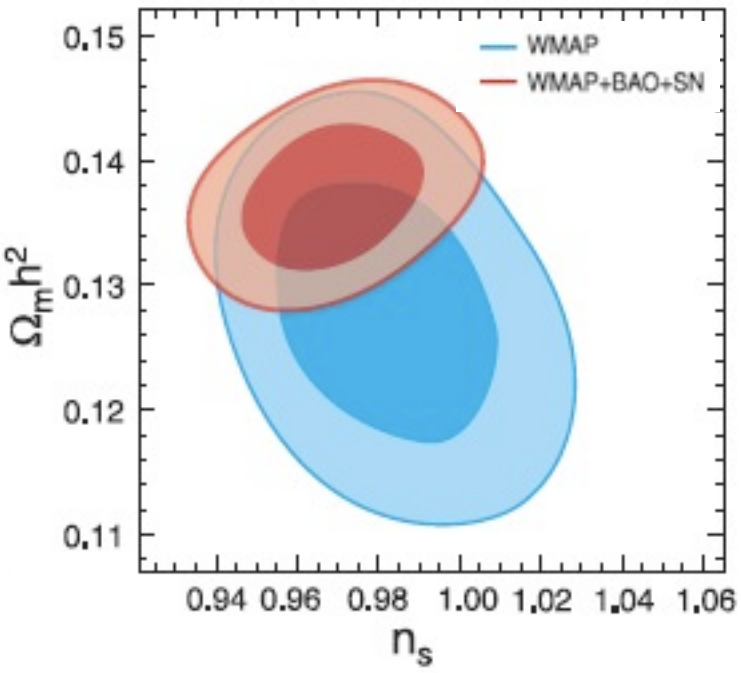

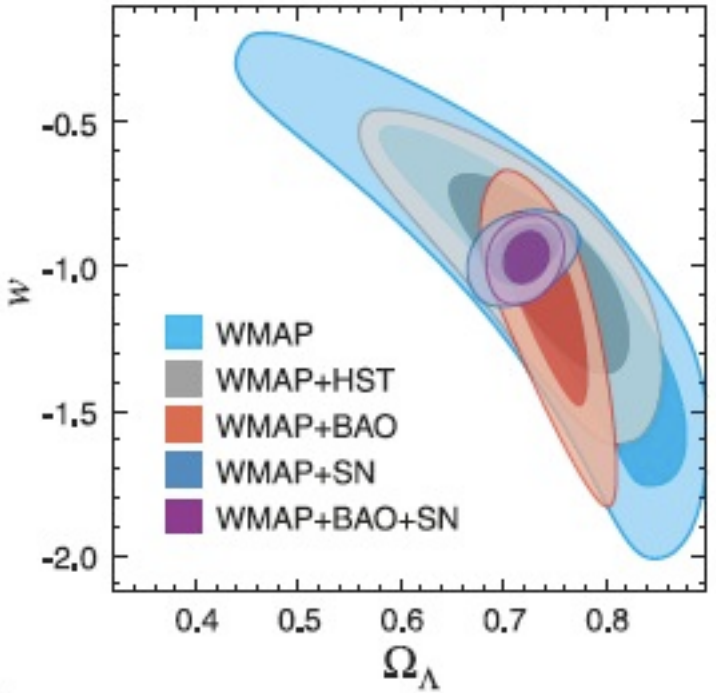

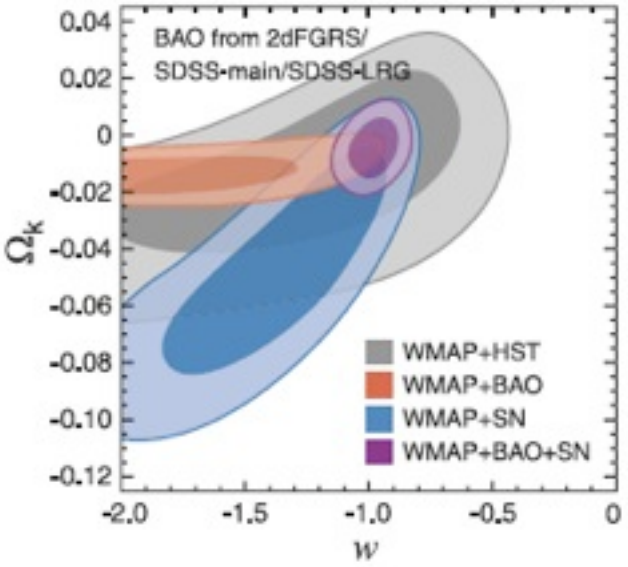

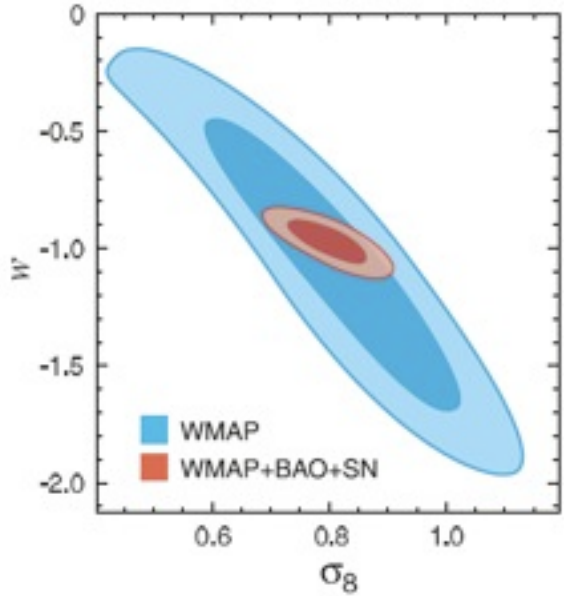

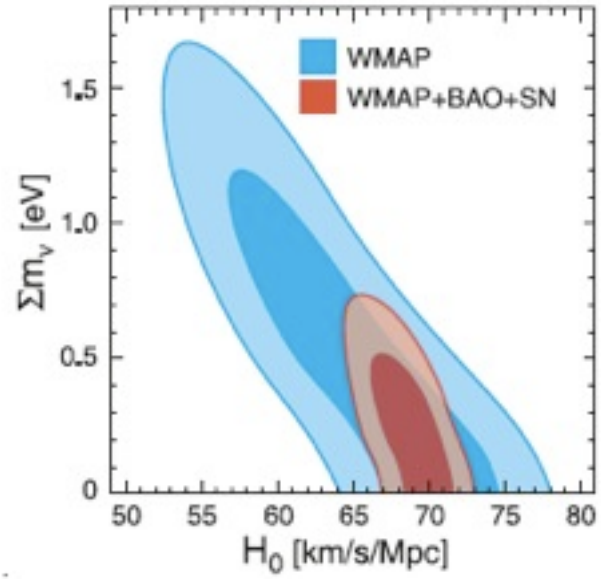

J. Dunkley, et.al. Five-Year Wilkinson Microwave Anisotropy Probe (WMAP) Observations: Likelihoods and Parameters from WMAP Data

Final paragraph of Conclusions:

Considering a range of extended models, we continue to find that **the standard ΛCDM model is consistently preferred by the data**. The improved measurement of the third peak now requires the existence of light relativistic species, assumed to be neutrinos, at high confidence. The standard scenario has three neutrino species, but the three-year WMAP data could not rule out models with none. **The CDM model also continues to succeed in fitting a substantial array of other observations.** Certain tensions between other observations and those of WMAP, such as the amplitude of matter fluctuations measured by weak lensing surveys and using the Ly-α forest, and the primordial lithium abundance, have either been resolved with improved understanding of systematics, or show promise of being explained by recent observations. With further WMAP observations we will better probe both the universe at a range of epochs, measuring fluctuation characteristics to probe the initial inflationary process, or other non-inflationary scenario, improving measurements of the composition of the universe at the recombination era, and characterizing the reionization process in the universe.

Outline

Cosmic Microwave Background
WMAP 5-year Data and Papers Released
Grand Unification of Forces
Phase Transitions in the Early Universe
Topological Defects: Strings, Monopoles*
Cosmic Inflation

*Note: I edited much of the material in the following Topological Defects slides from the website http://www.damtp.cam.ac.uk/user/gr/public/cs_top.html

Grand Unification

The basic premise of grand unification is that the known symmetries of the elementary particles result from a larger (and so far unknown) symmetry group G. Whenever a phase transition occurs, part of this symmetry is lost, so the symmetry group changes. This can be represented mathematically as

$$G \rightarrow H \rightarrow ... \rightarrow SU(3) \times SU(2) \times U(1) \rightarrow SU(3) \times U(1).$$

Here, each arrow represents a symmetry breaking phase transition where matter changes form and the groups - G, H, SU(3), etc. - represent the different types of matter, specifically the symmetries that the matter exhibits and they are associated with the different fundamental forces of nature.

The liquid phase of water is rotationally symmetric, that is, it looks the same around each point regardless of the direction in which we look. We could represent this large three-dimensional symmetry by the group G (actually SO(3)). The solid form of frozen water, however, is not uniform in all directions; the ice crystal has preferential lattice directions along which the water molecules align. The group describing these different discrete directions H, say, will be smaller than G. Through the process of freezing, therefore, the original symmetry G is broken down to H.

Grand Unified Theory

GUT refers to a theory in physics that unifies the strong interaction and electroweak interaction. Several such theories have been proposed, but none is currently universally accepted. The (future) theory that will also include gravity is termed theory of everything. Some common GUT models are:

- Georgi-Glashow (1974) model -- SU(5)
- SO(10)
- Flipped SU(5) -- SU(5)×U(1)
- Pati-Salam model -- SU(4)×SU(2)×SU(2)
- E_6

GUT models generically predict the existence of topological defects such as monopoles, cosmic strings, domain walls, and others. None have been observed and their absence is known as the monopole problem in cosmology.

There is still no hard evidence nature is described by a GUT theory. In fact, since the Higgs particle hasn't been discovered yet, it's not even certain if the Standard Model is fully accurate.

Topological Defects

These arise when some n-component scalar field $\phi_i(\mathbf{x}) = 0$ because of topological trapping that occurs as a result of a phase transition in the early universe (as I will explain shortly).

If the ϕ field is complex then n=2, and $\phi_i(\mathbf{x}) = 0$ occurs along a linear locus of points, a **string,** in three dimensional space. This corresponds to a 2-dimensional world-sheet in the 3+1 dimensions of spacetime.

If the ϕ field has three components, then $\phi_i(\mathbf{x}) = 0$ occurs at a point in three dimensional space, a **monopole**. This corresponds to a 1-dimensional world-line in the 3+1 dimensions of spacetime.

If the ϕ field has four components, then $\phi_i(\mathbf{x}) = 0$ occurs at a point in space-time, an **instanton**. A related concept is **texture**.

Phase transitions

The cosmological significance of symmetry breaking is due to the fact that symmetries are restored at high temperature (just as it is for liquid water when ice melts). For extremely high temperatures in the early universe, we will even achieve a grand unified state G. Viewed from the moment of creation forward, the universe will pass through a sucession of phase transitions at which the strong nuclear force will become differentiated and then the weak nuclear force and electromagnetism.

Phase transitions can have a wide variety of important implications including the formation of topological defects -cosmic strings, domain walls, monopoles and textures, or it may even trigger a period of exponential expansion (inflation).

Phase transitions can be either dramatic - first order - or smooth - second order.

During a first-order phase transition, the matter fields get trapped in a `false vacuum' state from which they can only escape by nucleating bubbles of the new phase, that is, the `true vacuum' state.

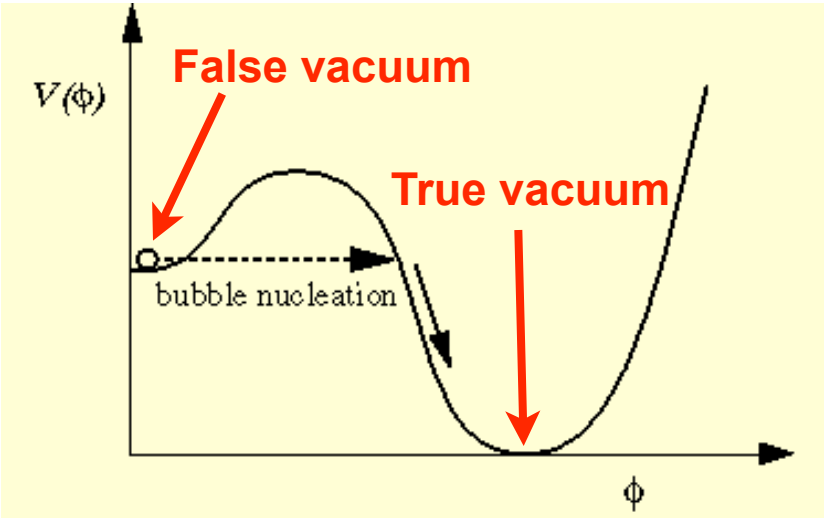

First-order phase transitions (illustrated below) occur through the formation of bubbles of the new phase in the middle of the old phase; these bubbles then expand and collide until the old phase disappears completely and the phase transition is complete.

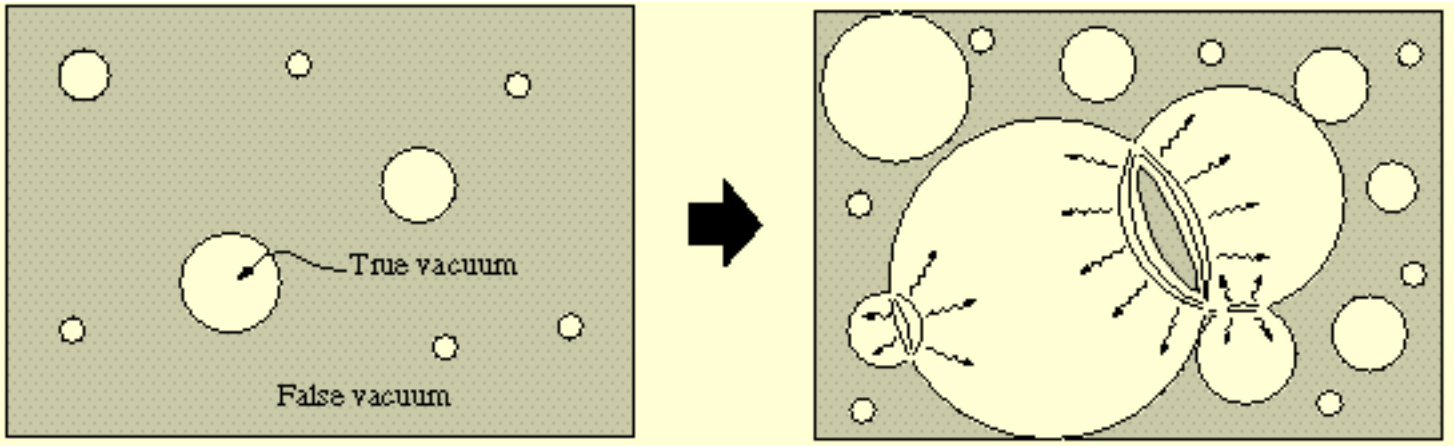

First-order phase transitions proceed by bubble nucleation. A bubble of the new phase (the true vacuum) forms and then expands until the old phase (the false vacuum) disappears. A useful analogue is boiling water in which bubbles of steam form and expand as they rise to the surface.

Second-order phase transitions, on the other hand, proceed smoothly. The old phase transforms itself into the new phase in a continuous manner. There is energy (specific heat of vaporization, for example) associated with a first order phase transition.

Either type of phase transition can produce stable configurations called “topological defects.”

Cosmic Strings & Other Topological Defects

Topological defects are stable configurations that are in the original, symmetric or old phase, but nevertheless for topological reasons they persist after a phase transition to the asymmetric or new phase is completed - because to unwind them would require a great deal of energy. There are a number of possible types of defects, such as domain walls, cosmic strings, monopoles, and textures. The type of defect is determined by the symmetry properties of the matter and the nature of the phase transition.

Domain walls: These are two-dimensional objects that form when a discrete symmetry is broken at a phase transition. A network of domain walls effectively partitions the universe into various `cells'. Domain walls have some rather peculiar properties. For example, the gravitational field of a domain wall is repulsive rather than attractive.

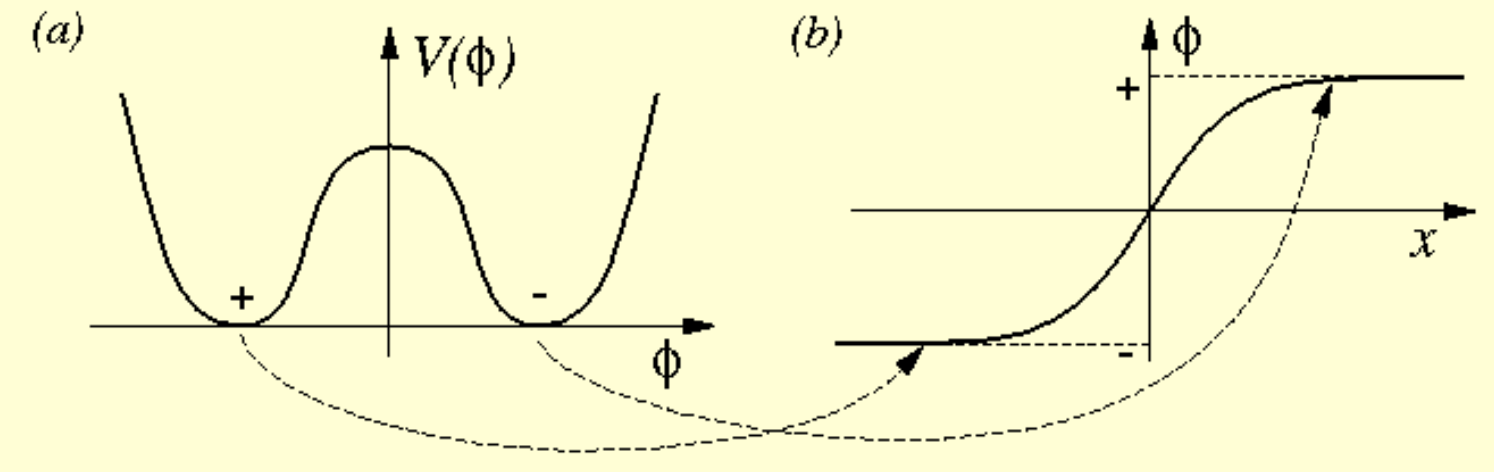

Cosmic strings: These are one-dimensional (that is, line-like) objects which form when an axial or cylindrical symmetry is broken. Strings can be associated with grand unified particle physics models, or they can form at the electroweak scale. They are very thin and may stretch across the visible universe. A typical GUT string has a thickness that is less then a trillion times smaller that the radius of a hydrogen atom, but a 10 km length of one such string would weigh as much as the earth itself!

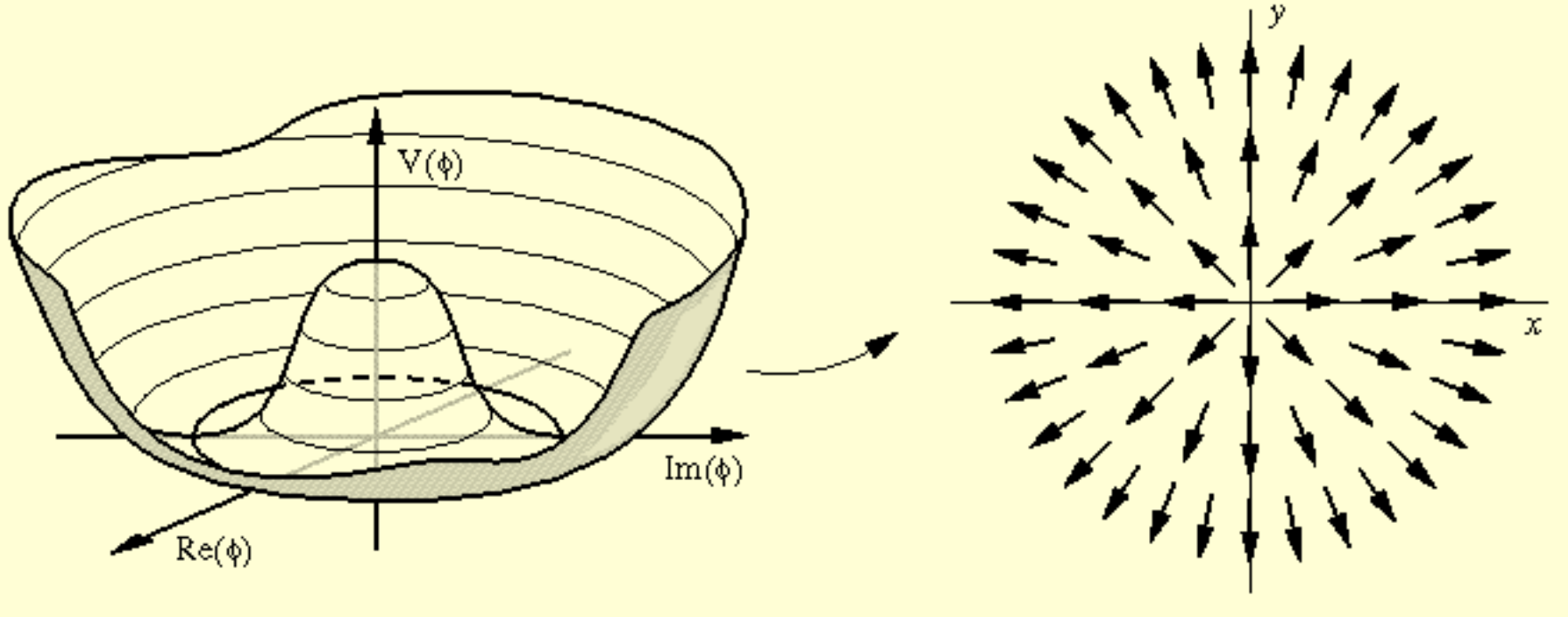

Cosmic strings are associated with models in which the set of minima are not simply-connected, that is, the vacuum manifold has `holes' in it. The minimum energy states on the left form a circle and the string corresponds to a non-trivial winding around this.

Monopoles: These are zero-dimensional (point-like) objects which form when a spherical symmetry is broken. Monopoles are predicted to be supermassive and carry magnetic charge. The existence of monopoles is an inevitable prediction of grand unified theories (GUTs - more on this shortly); why the universe isn't filled with them is one of the puzzles of the standard cosmology.

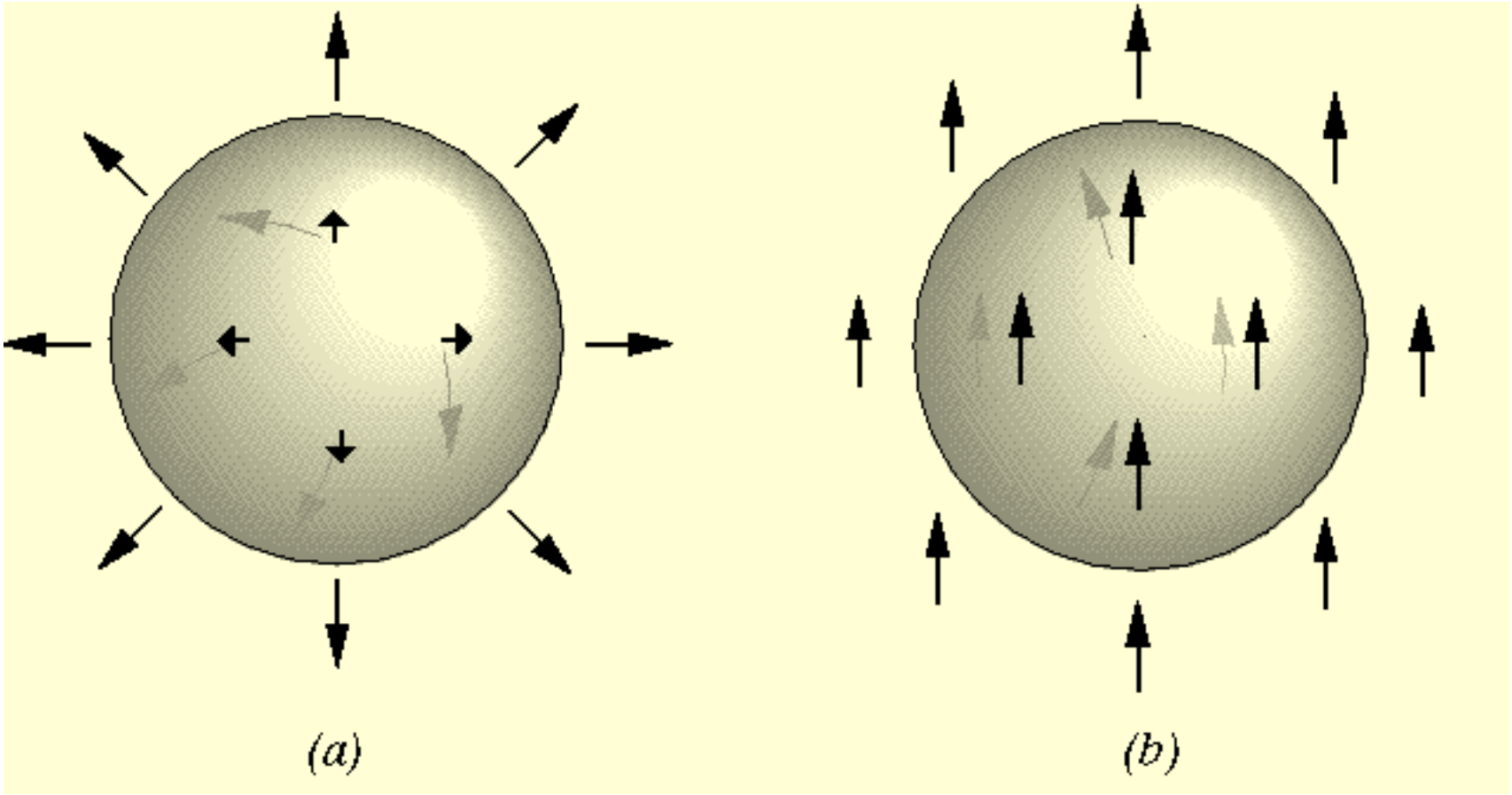

Textures: These form when larger, more complicated symmetry groups are completely broken. Textures are delocalized topological defects which are unstable to collapse. A speculation that the largest “cold spot” in the WMAP CMB data was caused by cosmic textures was published by Cruz et al. (2007, Science 318, 1612).

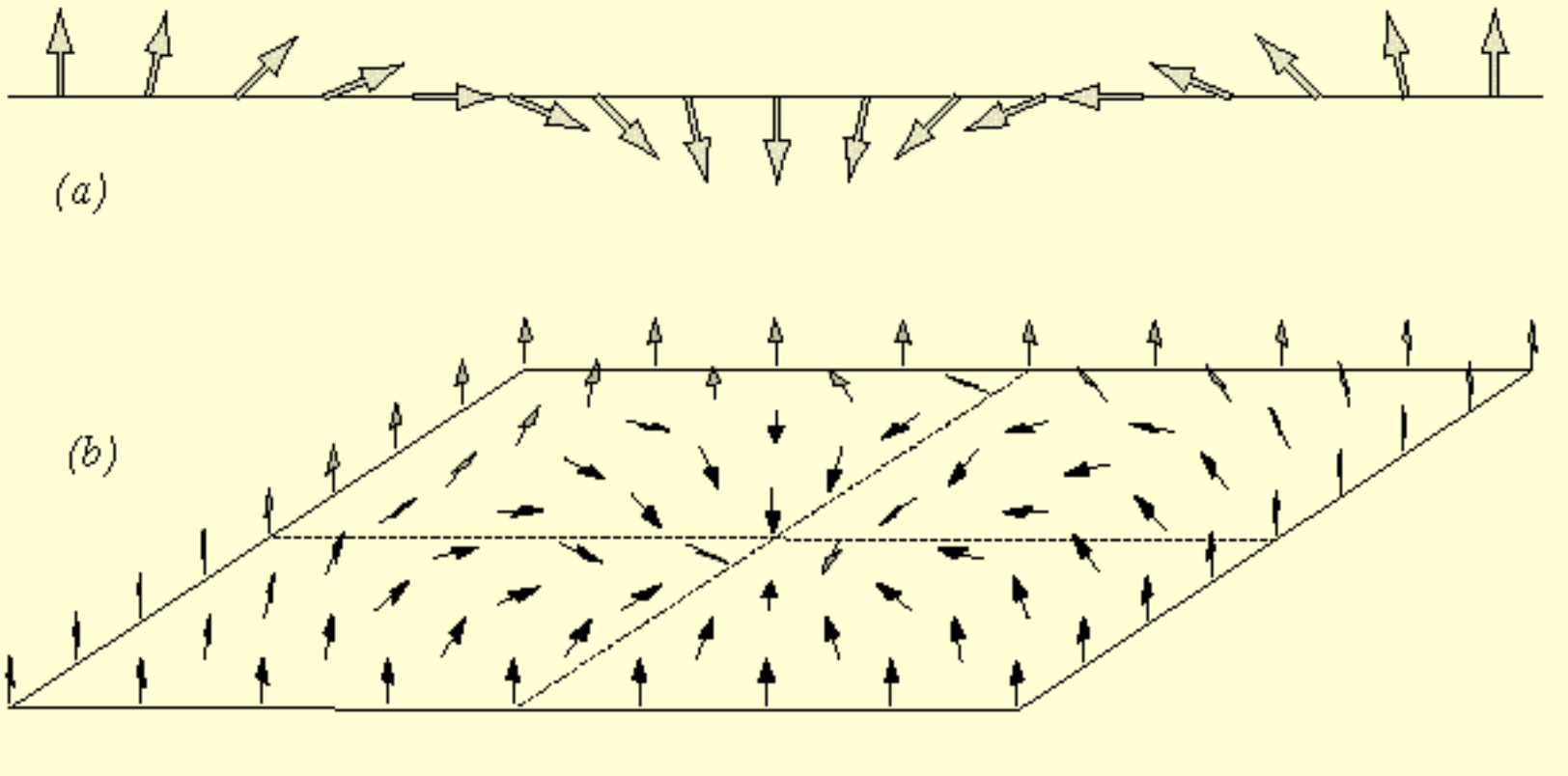

Examples of delocalized texture configurations in one and two dimensions.

CMB Lensing and the WMAP Cold Spot

Sudeep Das[1,*] and David N. Spergel[1,2,3,†]

Cosmologists have suggested a number of intriguing hypotheses for the origin of the "WMAP cold spot", the coldest extended region seen in the CMB sky, including a very large void and a collapsing texture. Either hypothesis predicts a distinctive CMB lensing signal. We show that the upcoming generation of high resolution CMB experiments such as ACT and SPT should be able to detect the signatures of either textures or large voids. If either signal is detected, it would have profound implications for cosmology.

Some theorists have speculated that the Cold Spot is a secondary effect, generated at some intermediate distance between us and the last scattering surface. One such model proposes that the Cold Spot may have been caused by the Rees-Sciama effect due to an underdense void of comoving radius $\sim 200h^{-1}$Mpc and fractional density contrast $\delta \sim -0.3$ at redshift of $z < 1$ [8, 9]. Interestingly, [10] reported a detection of an underdense region with similar characteristics in the distribution of extragalactic radio sources in the NRAO VLA Sky Survey in the direction of the Cold Spot, a claim which has recently been challenged [11]. An alternative view [12] proposes that the spot was caused by the interaction of the CMB photons with a cosmic texture, a type of topological defect that can give rise to hot and cold spots in the CMB [13]. Bayesian analysis by [14] claims that the texture hypothesis seems to be favored over the void explanation, mainly because such large voids as required by the latter is highly unlikely to form in a CDM structure formation scenario.

[8] K. T. Inoue and J. Silk, ApJ 648, 23 (2006), arXiv:astroph/ 0602478.
[9] K. T. Inoue and J. Silk, ApJ 664, 650 (2007), arXiv:astro-ph/0612347.
[10] L. Rudnick, S. Brown, and L. R. Williams, ApJ 671, 40 (2007).
[11] K. M. Smith and D. Huterer, ArXiv:0805.2751.
[12] M. Cruz, N. Turok, P. Vielva, E. Mart´ınez-Gonz´alez, and M. Hobson, Science 318, 1612 (2007).
[13] N. Turok and D. Spergel, Physical Review Letters 64, 2736 (1990).
[14] M. Cruz, E. Martinez-Gonzalez, P. Vielva, J. M. Diego, M. Hobson, and N. Turok, ArXiv:0804.2904.

A Cosmic Microwave Background Feature Consistent with a Cosmic Texture

M. Cruz,[1,2]* N. Turok,[3] P. Vielva,[1] E. Martínez-González,[1] M. Hobson[4]
SCIENCE VOL 318 7 DECEMBER 2007

The Cosmic Microwave Background provides our most ancient image of the universe and our best tool for studying its early evolution. Theories of high-energy physics predict the formation of various types of topological defects in the very early universe, including cosmic texture, which would generate hot and cold spots in the Cosmic Microwave Background. We show through a Bayesian statistical analysis that the most prominent 5°-radius cold spot observed in all-sky images, which is otherwise hard to explain, is compatible with having being caused by a texture. From this model, we constrain the fundamental symmetry-breaking energy scale to be $\phi_0 \approx 8.7 \times 10^{15}$ gigaelectron volts. If confirmed, this detection of a cosmic defect will probe physics at energies exceeding any conceivable terrestrial experiment.

The Axis of Evil revisited

Kate Land, Joao Magueijo, 2007 MNRAS, 378, 153

Abstract: In light of the three-year data release from WMAP we re-examine the evidence for the ``Axis of Evil'' (AOE) [anomalous alignment of CMB multipoles in the direction l ≃ –100, b = 60]. We discover that previous statistics are not robust with respect to the data-sets available and different treatments of the galactic plane. We identify the cause of the instability and implement an alternative ``model selection'' approach. A comparison to Gaussian isotropic simulations find the features significant at the 94-98% level, depending on the particular AOE model. The Bayesian evidence finds lower significance, ranging from ``substantial'' to no evidence for the most general AOE model.

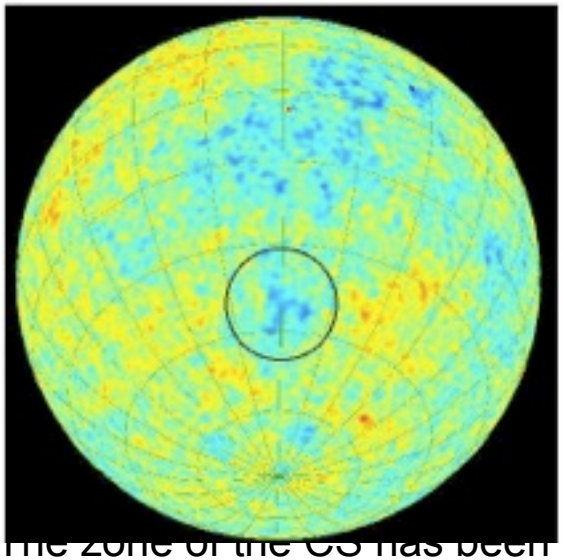

The zone of the CS has been placed at the center of the black circle.

MNRAS 390, 913 (2008)

The CMB cold spot: texture, cluster or void?

M. Cruz,[1⋆] E. Martínez-González,[1] P. Vielva,[1] J. M. Diego,[1] M. Hobson,[2] N. Turok[3]

The non-Gaussian cold spot found in the WMAP data has created controversy about its origin. Here we calculate the Bayesian posterior probability ratios for three different models that could explain the cold spot. A recent work claimed that the Spot could be caused by a cosmic texture, while other papers suggest that it could be due to the gravitational effect produced by an anomalously large void. Also the Sunyaev-Zeldovich effect caused by a cluster is taken into account as a possible origin. We perform a template fitting on a 20° radius patch centered at Galactic coordinates $(b = -57^{\circ}, l = 209^{\circ})$ and calculate the posterior probability ratios for the void and Sunyaev-Zeldovich models, comparing the results to those obtained with texture. Taking realistic priors for the parameters, the texture interpretation is favored, while the void and Sunyaev-Zeldovich hypotheses are discarded. The temperature decrement produced by voids or clusters is negligible considering realistic values for the parameters.

Why do cosmic topological defects form?

If cosmic strings or other topological defects *can* form at a cosmological phase transition then they *will* form. This as first pointed out by Kibble and, in a cosmological context, the defect formation process is known as the **Kibble mechanism**.

The simple fact is that causal effects in the early universe can only propagate (as at any time) as the speed of light c. This means that at a time t, regions of the universe separated by more than a distance $d=ct$ can know nothing about each other. In a symmetry breaking phase transition, different regions of the universe will choose to fall into different minima in the set of possible states (this set is known to mathematicians as the vacuum manifold). Topological defects are precisely the "boundaries" between these regions with different choices of minima, and their formation is therefore an inevitable consequence of the fact that different regions cannot agree on their choices.

For example, in a theory with two minima, plus + and minus -, then neighbouring regions separated by more than ct will tend to fall randomly into the different states (as shown below). Interpolating between these different minima will be a **domain wall**.

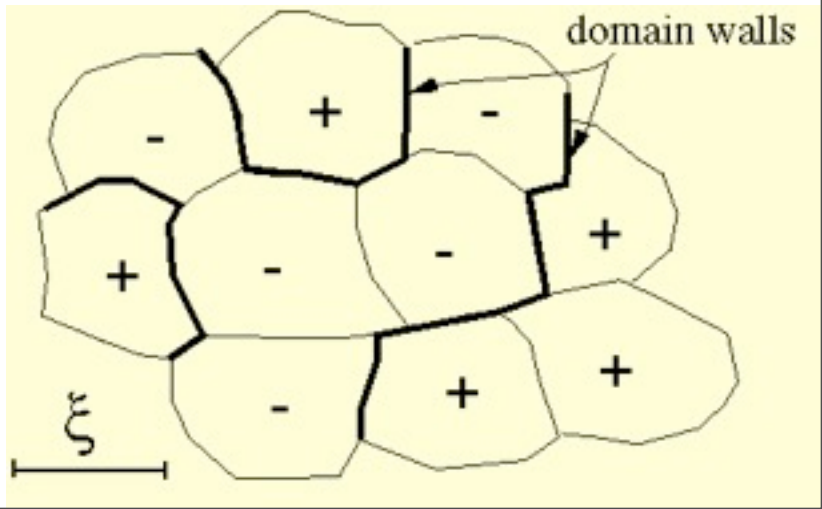

Cosmic strings will arise in slightly more complicated theories in which the minimum energy states possess `holes'. The strings will simply correspond to non-trivial `windings' around these holes (as illustrated at right).

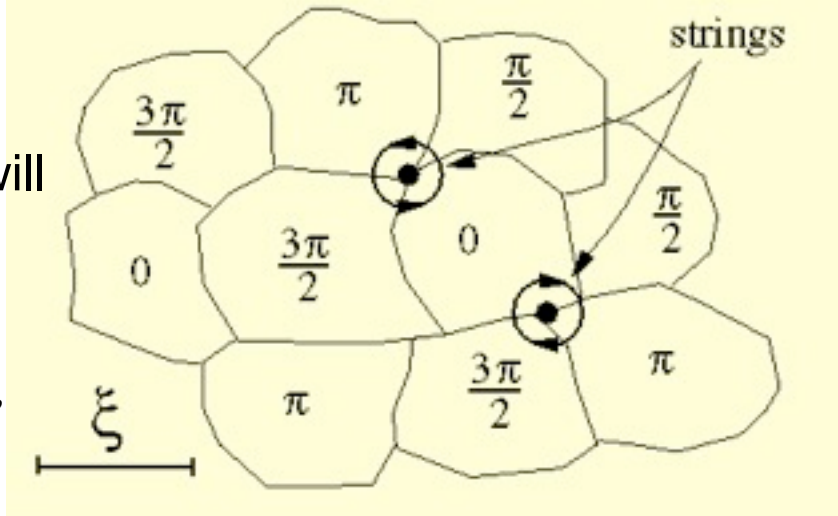

The Kibble mechanism for the formation of cosmic strings.

Topological defects can provide a unique link to the physics of the very early universe. Furthermore, they can crucially affect the evolution of the universe, so their study is an unavoidable part of any serious attempt to understand the early universe. The **cosmological consequences** very with the type of defect considered. Domain walls and monopoles are cosmologically catastrophic. Any cosmological model in which they form will evolve in a way that contradicts the basic observational facts that we know about the universe. Such models must therefore be ruled out! Cosmic inflation was invented to solve this problem.

Cosmic strings and textures are (possibly) much more benign. Among other things, the were until recently thought to be a possible source of the fluctuations that led to the formation of the large-scale structures we observe today, as well as the anisotropies in the Cosmic Microwave Background. However, the CMB anisotropies have turned out not to agree with the predictions of this theory.

Cosmic String Dynamics and Evolution

The evolution of cosmic string network is the relatively complicated result of only three rather simple and fundamental processes: cosmological expansion, intercommuting & loop production, and radiation.

Cosmological expansion

The overall expansion of the universe will ‘stretch’ the strings, just like any other object that is not gravitationally bound. You can easily undertand this through the well-known analogy of the expanding balloon. If you draw a line of the surface of the balloon and then blow it up, you will see that the length of your `string' will grow at the same rate as the radius of the balloon.

Intercommuting & loop production

Whenever two long strings cross each other, they exchange ends, or `intercommute' (case (a) in the figure below). In particular, a long string can intercommute with itself, in which case a loop will be produced (this is case (b) below).

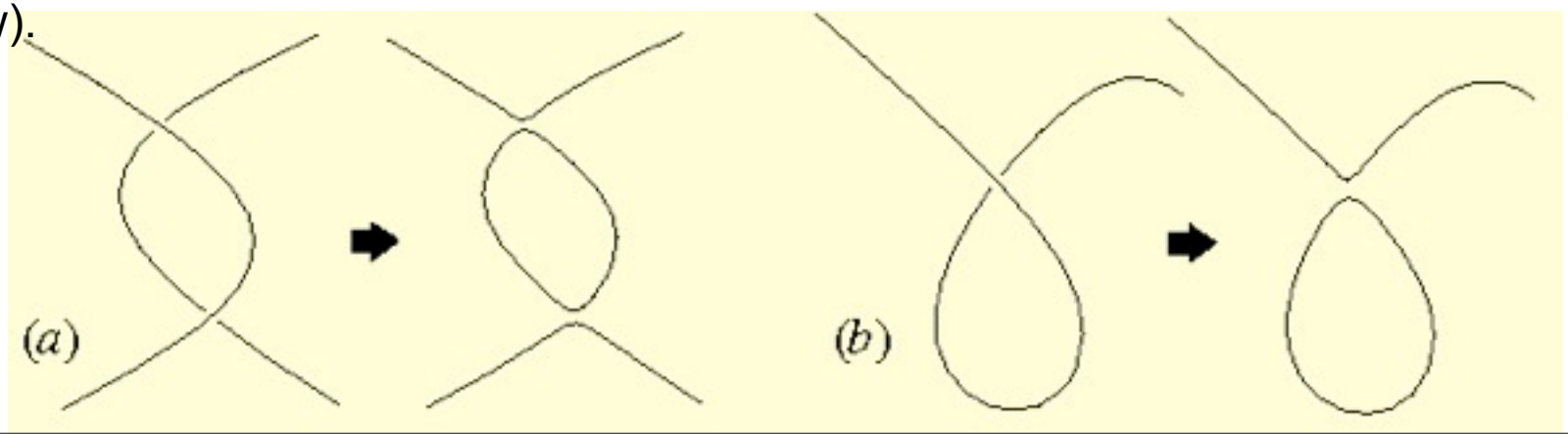

Radiation from strings

Both long cosmic strings and small loops will emit radiation. In most cosmological scenarios this will be **gravitational radiation**, but electromagnetic radiation or axions can also be emitted in some cases (for some specific phase transitions).

The effect of radiation is much more dramatic for loops, since they lose all their energy this way, and eventually disappear. Here you can see what happens in the case of two interlocked loops. This configuration is unlikely to happen in a cosmological setting, but it is nevertheless quite enlightening. Notice the succession of complicated dynamic processes before the loop finally disappears!

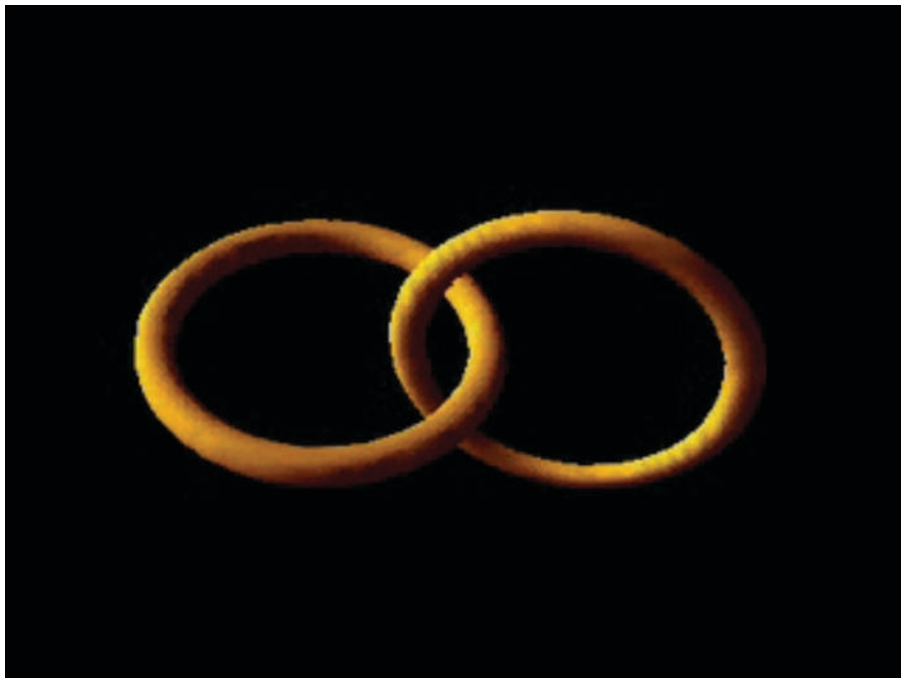

After formation, an initially high density string network begins to chop itself up by producing small loops. These loops oscillate rapidly (relativistically) and decay away into gravitational waves.

The net result is that the strings become more and more dilute with time as the universe expands. From an enormous density at formation, mathematical modelling suggests that today there would only be about 10 long strings stretching across the observed universe, together with about a thousand small loops!

In fact the network dynamics is such that the string density will eventually stabilize at an exactly constant level relative to the rest of the radiation and matter energy density in the universe. Thus the string evolution is described as **`scaling'** or scale-invariant, that is, the properties of the network look the same at any particular time t if they are scaled (or multiplied) by the change in the time. This is schematically represented below:

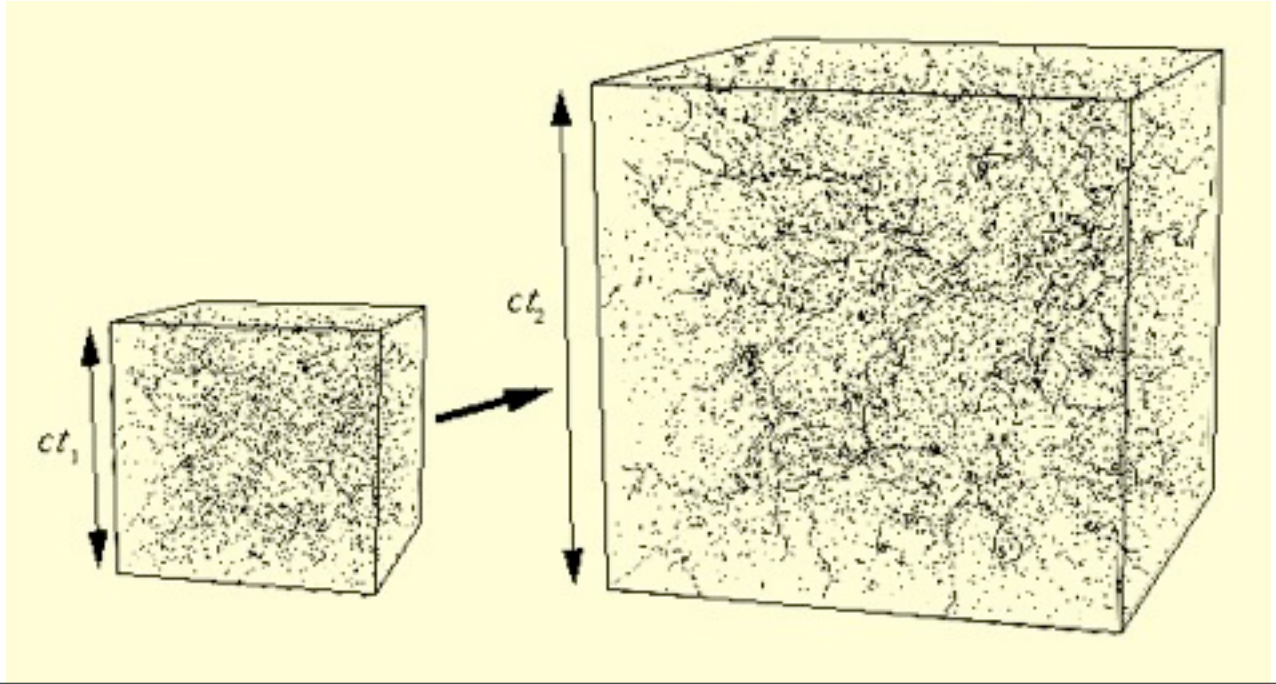

Because strings are extremely complex non-linear objects, the only rigorous way to study their evolution and cosmological consequences is to simulate in on the computer. One of the aims of performing numerical simulations of the evolution of cosmic string networks is to subsequently use the resulting information as an input to build (relatively) simpler semianalytic models that reproduce (in an averaged sense) the crucial properties of these objects. One starts by generating an initial “box of stings” containing a configuration of strings such as one would expect to find after a phase transition in the early universe. Then one evolves this initial box, by using the laws of motion of the strings.

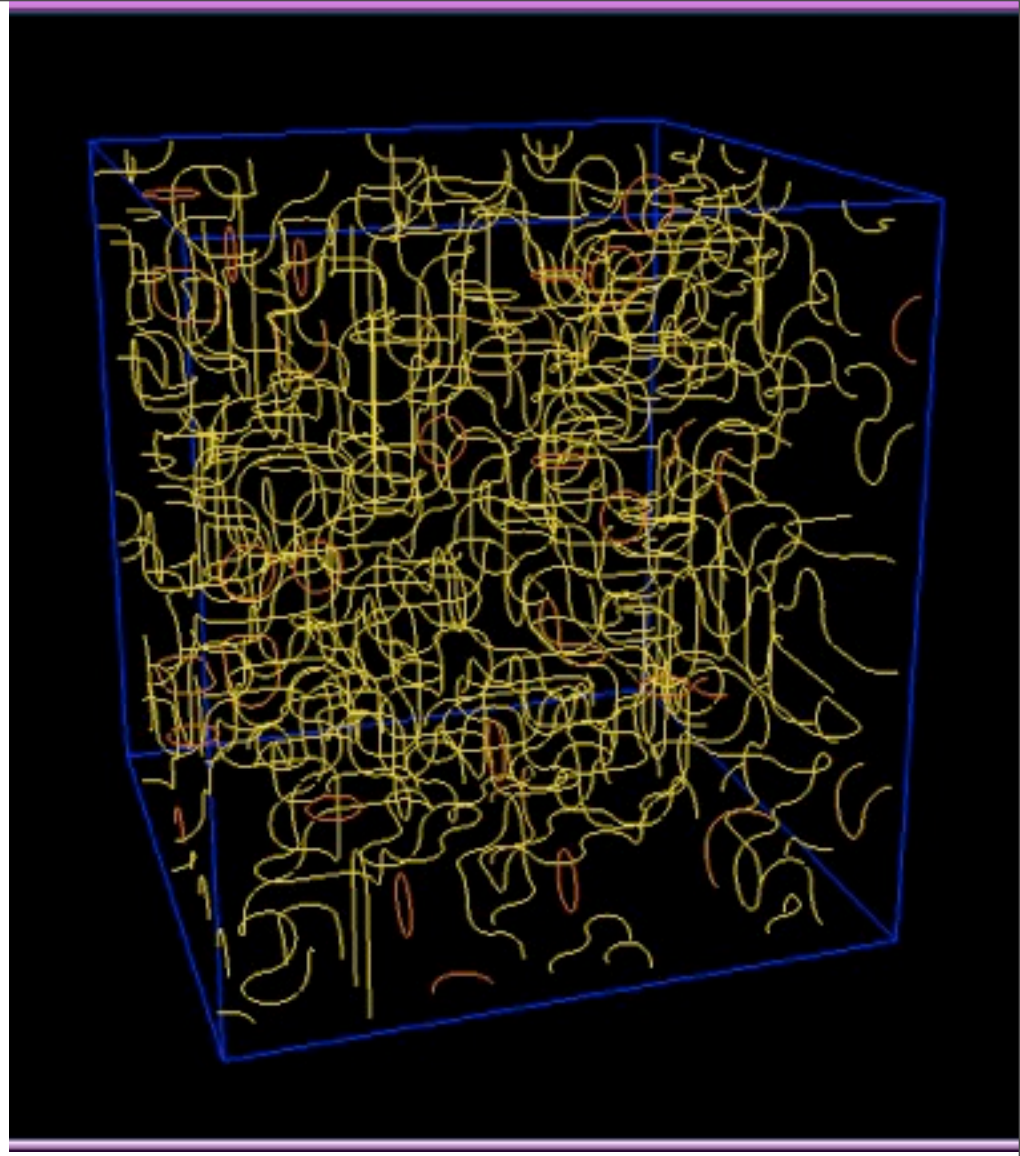

In this and all other pictures and movies below long strings are shown in yellow, while small loops have a color code going from yellow to red according to their size (red loops being the smallest).

Why do the two boxes below look different? Because the rate at which the universe is expanding is different.

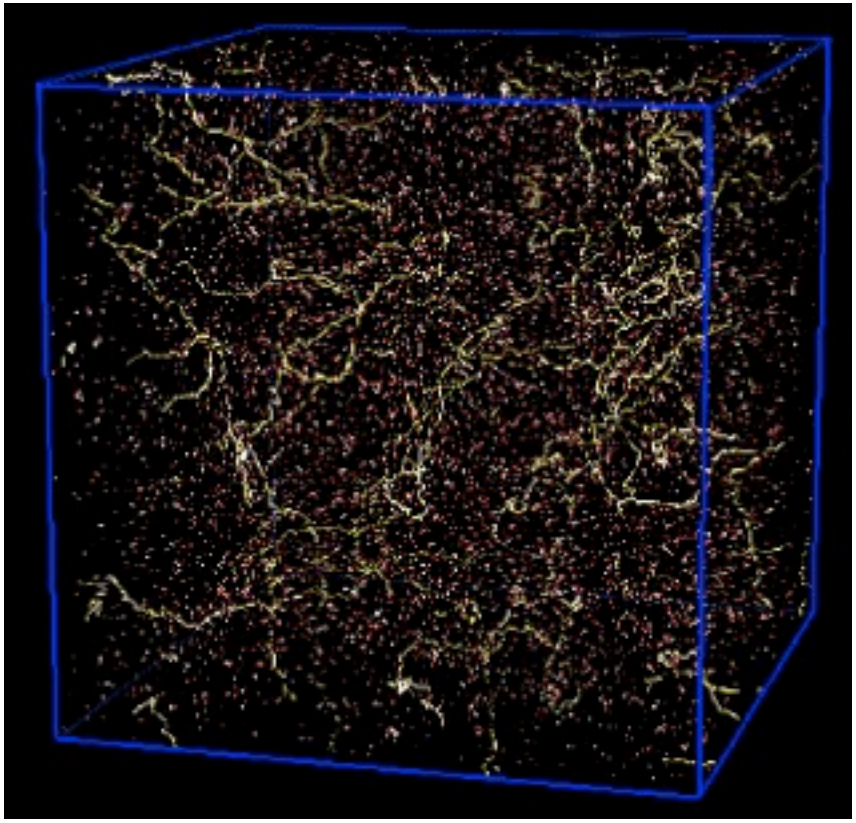

Snapshot of a string network in the radiation era. Note the high density of small loops and the `wiggliness' of the long strings in the network. The box size is about 2ct. (B. Allen & E. P. Shellard)

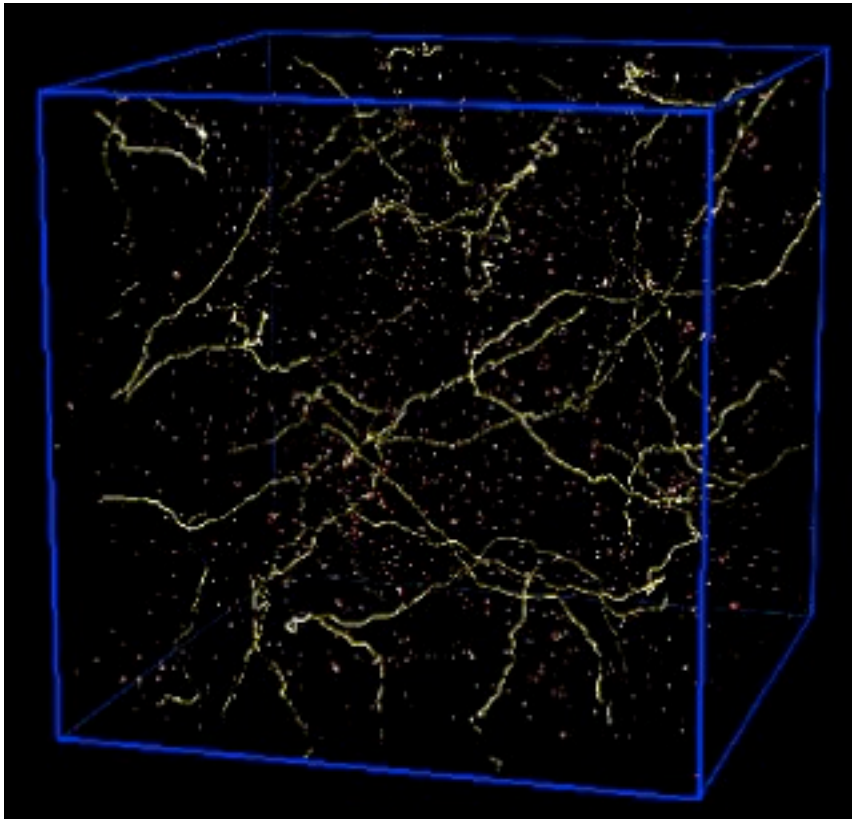

Snapshot of a string network in the matter era. Compare with the radiation case at left. Notice the lower density of both long strings and loops, as well as the lower `wiggliness' of the former. The box size is again about 2ct.

Two movies of the evolution of a cosmic string network in the radiation era. In the movie on the left the box has a fixed size (so you will see fewer and fewer strings as it evolves), while in the one on the right it grows as the comoving horizon. (C. Martins & E. P. Shellard)

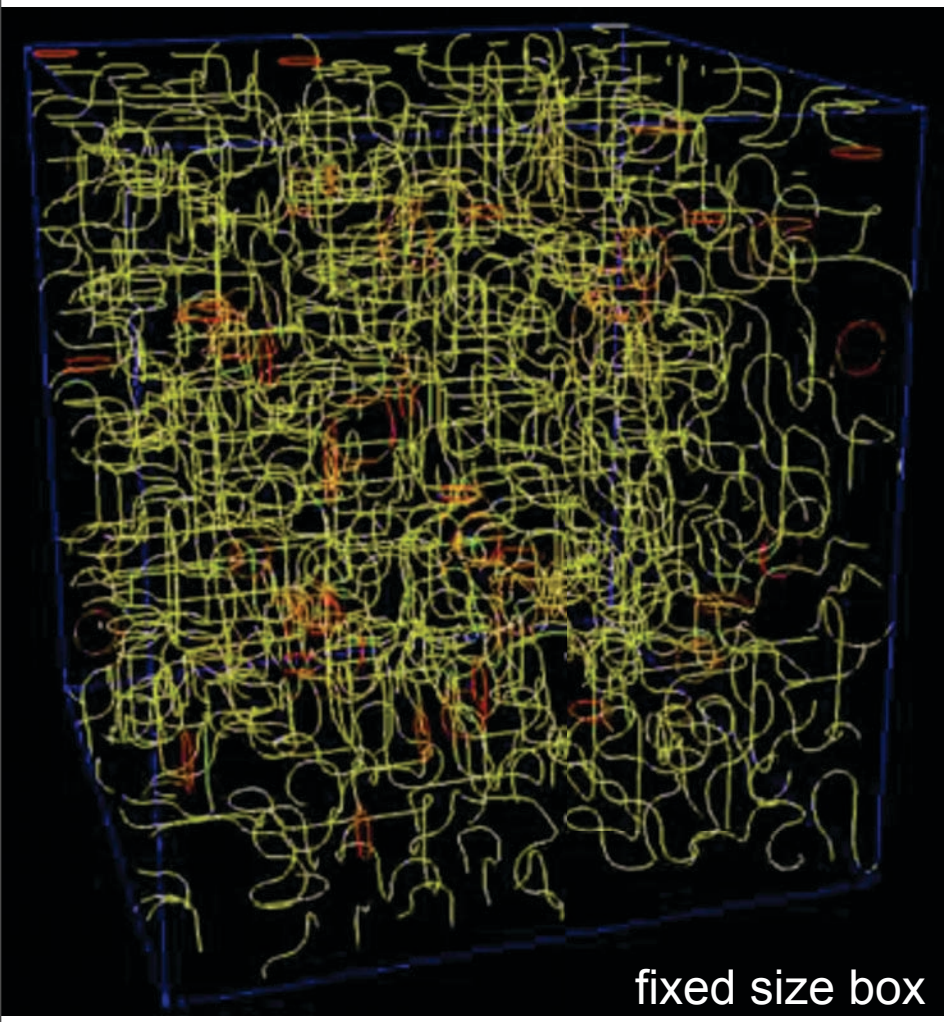

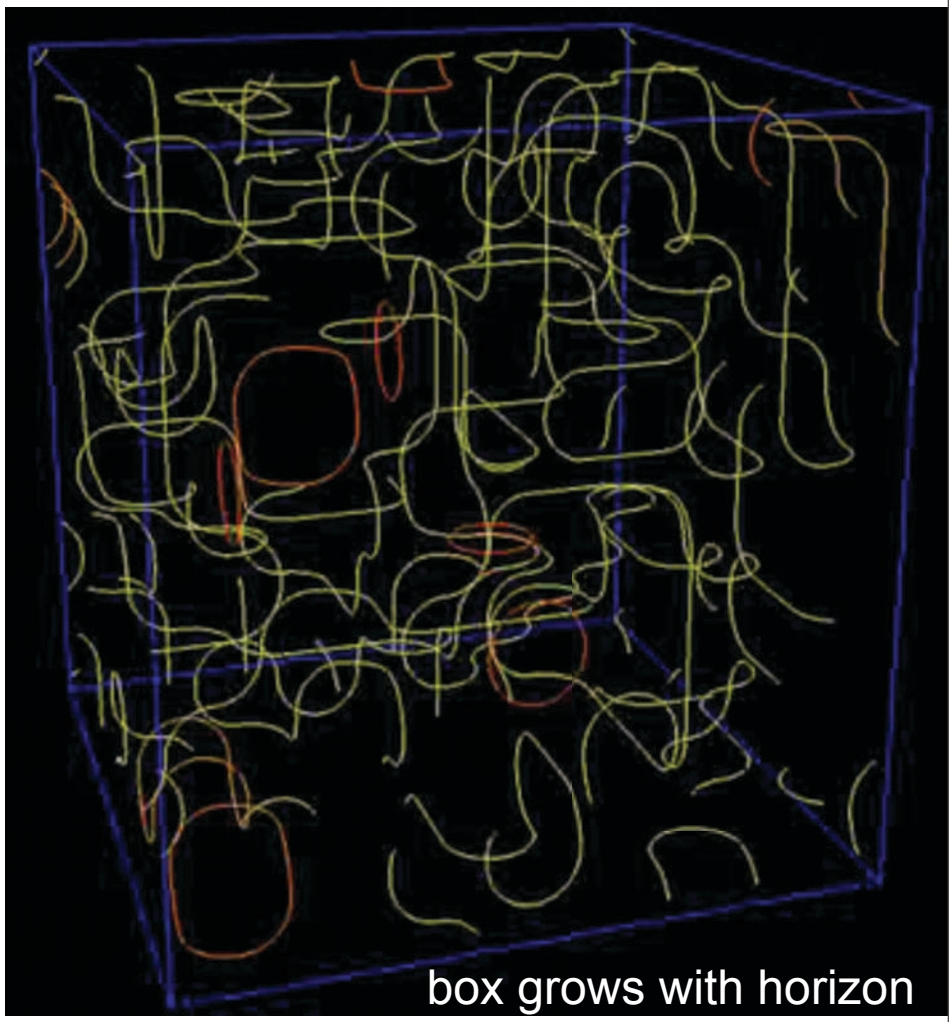

Notice that the number of long strings in the box that grows with the horizon remains roughly constant, in agreement with the scaling hypothesis. This is because the additional length in strings is quickly converted into small loops.

Two movies of the evolution of a cosmic string network in the matter era. In the movie on the left the box has a fixed size (so you will see fewer and fewer strings as it evolves), while in the one on the right it grows as the comoving horizon. (C. Martins & E. P. Shellard)

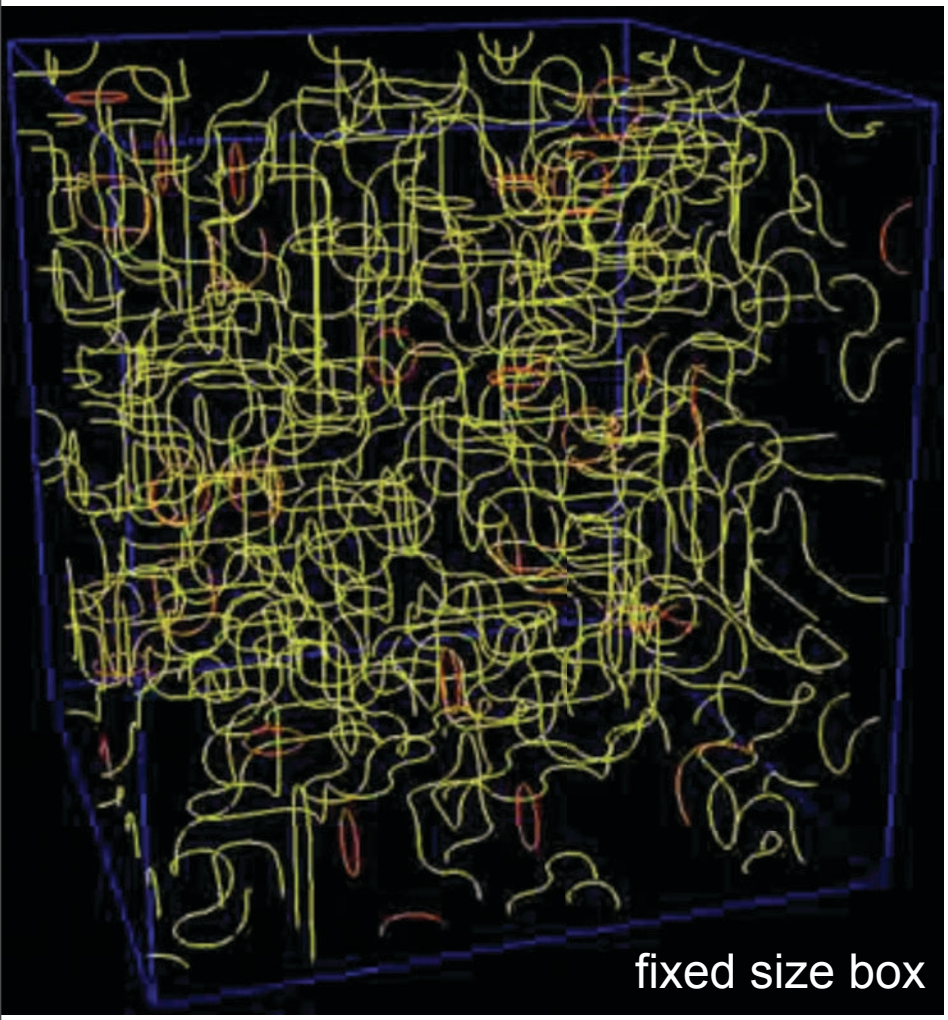

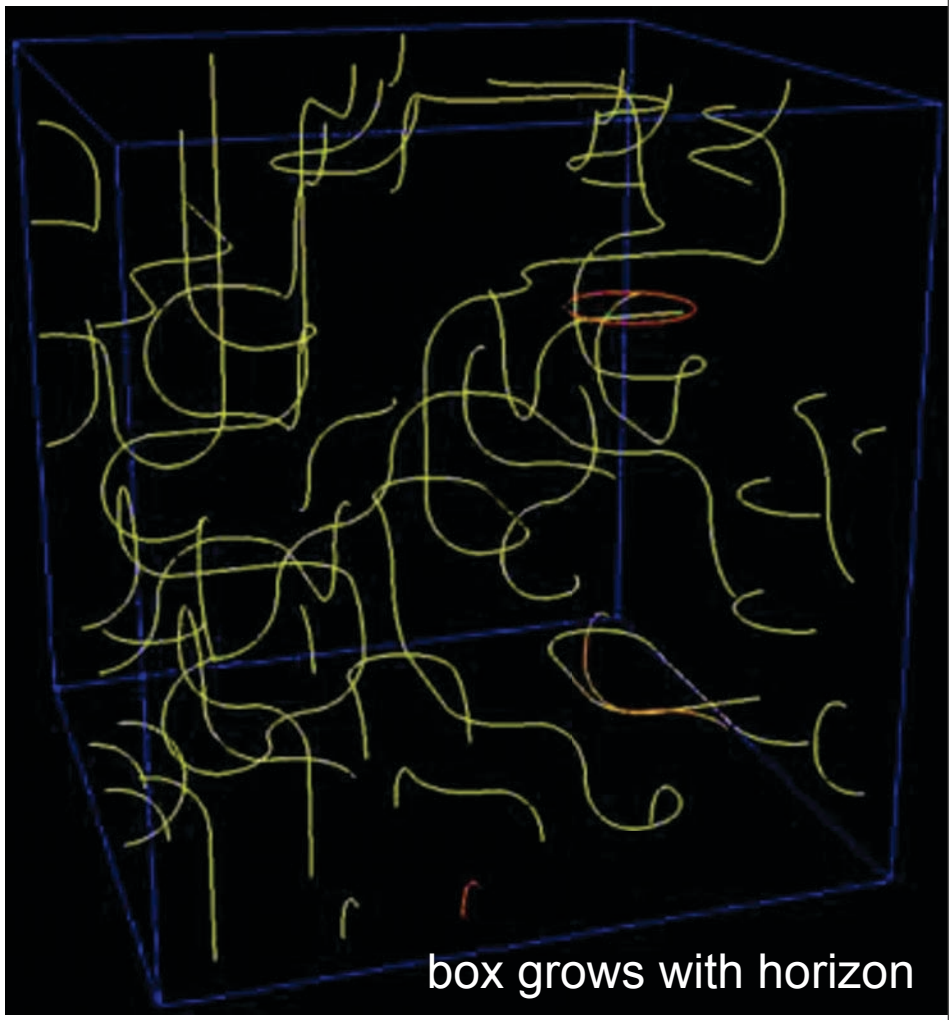

Notice that the number of long strings in the box that grows with the horizon again remains roughly constant, in agreement with the scaling hypothesis. This is because the additional length in strings is quickly converted into

When strings evolve, scaling from smaller scales to larger ones, they create perturbations in the matter energy density of the universe. Because of their tension, cosmic strings pull straight as they come inside the horizon. Although there is no gravitational force from a static string, such moving cosmic strings produce wakes toward which matter falls, thus serving as seeds for structure formation. For a static string along the z axis of mass μ per unit length, the energy momentum tensor is

$$T^{\mu\nu} = \mu\,\mathrm{diag}(1,0,0,-1)\delta(x)\delta(y)$$

and the metric is

$$\mathrm{d}s^2 = \mathrm{d}t^2 - \mathrm{d}z^2 - \mathrm{d}R^2 - (1-4G\mu)^2 R^2 \mathrm{d}\varphi^2$$

$G\mu \approx (M_{GUT}/M_{Pl})^2 \approx 10^{-6}$ is just the magnitude needed for GUT string structure formation. There is an angular defect of $8\pi G\mu = 5.18''$ (10^6 Gμ). This implies that the geodesic path of light is curved towards a string when light passes by it. Two copies of a galaxy near a cosmic string will appear to observers on the other side of the string.

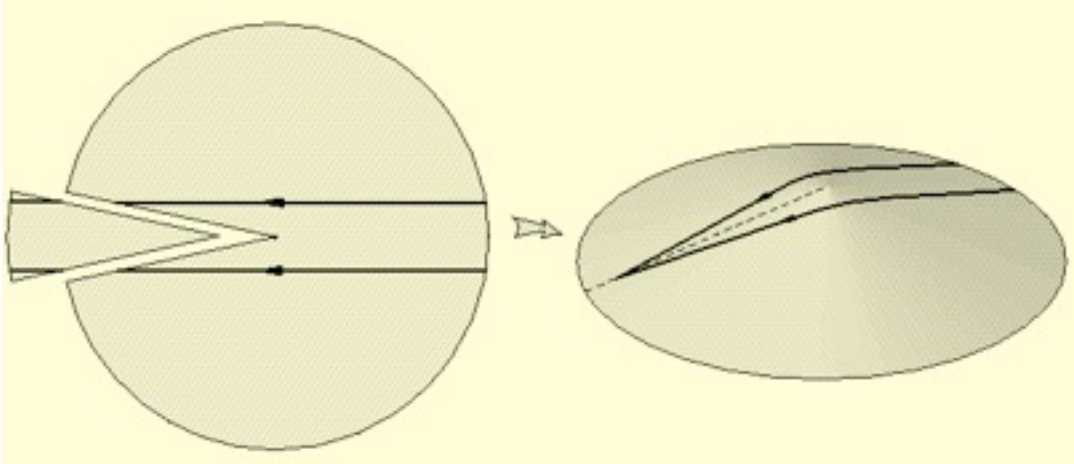

A. Vilenkin, E. P. S. Shellard, **Cosmic Strings and Other Topological Defects** (Cambridge U P, 1994)

Cosmic Strings Summary

Cosmic strings arise in spontaneously broken (SB) gauge theories

$$\mathcal{L} = -\tfrac{1}{4} F_{\mu\nu} F^{\mu\nu} - |\partial_\mu \phi|^2 - \lambda\left(|\phi|^2 - \phi_v^2\right)^2$$

as a consequence of causality in the expanding universe.

As the temperature T falls, a complex scalar field ϕ gets a nonzero expectation value

$$\phi(x) = \phi_v \, e^{\,i\theta(x)}$$

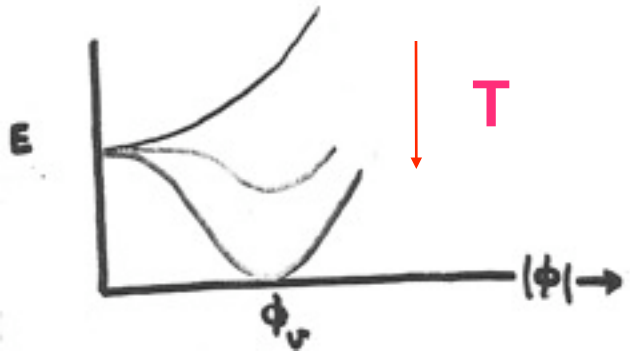

The phase θ will inevitably be different in regions separated by distances greater than the horizon size when the SB phase transition occurred.

If θ runs over $0 \rightarrow 2\pi$ as x goes around a loop in space, the loop encloses a string.

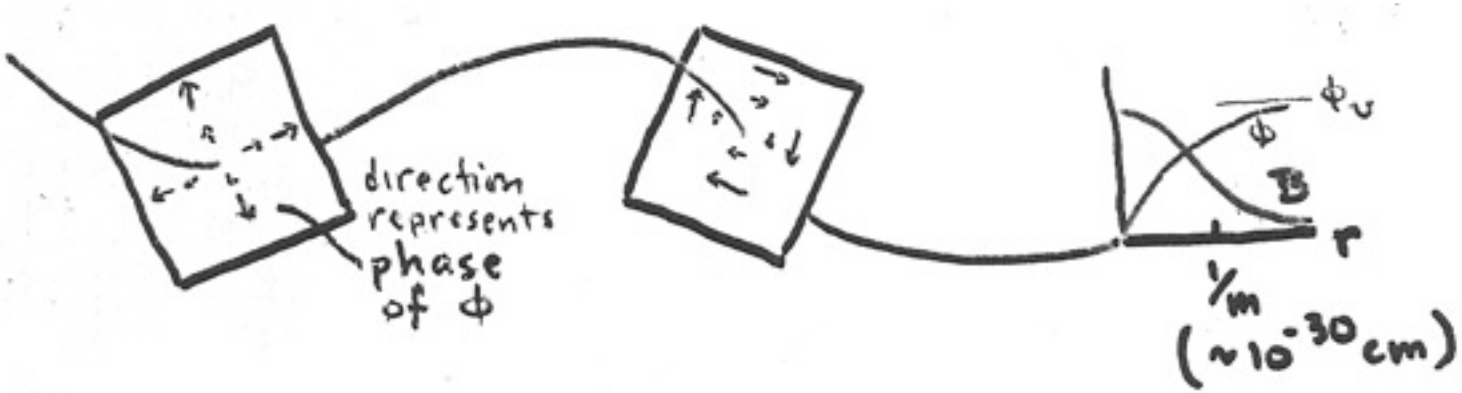

By 2000, it was clear that **cosmic defects are not the main source of the CMB anisotropies**.

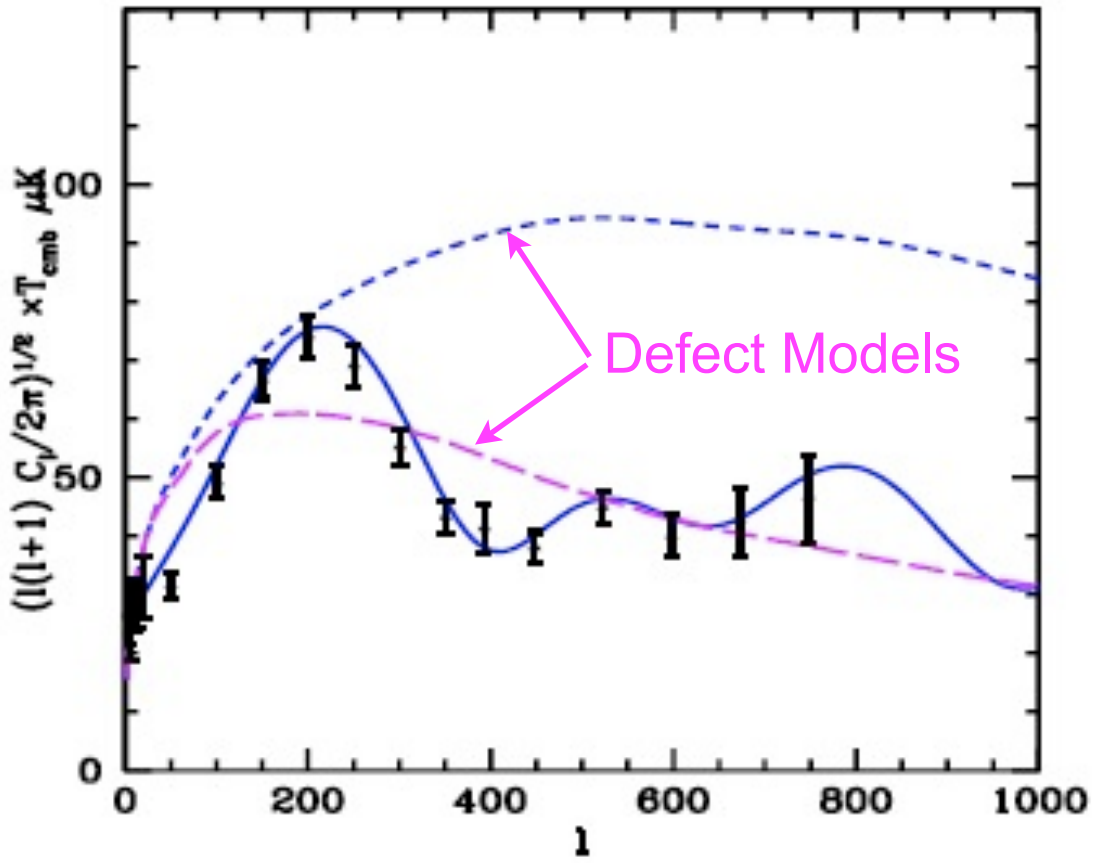

Figure 3: Current data (as complied by Knox[22]) with two defect models (dashed) and an inflation-based model (solid). The upper defect model has a standard ionization history and the lower model has an ionization history specifically designed to produce a sharper, shifted peak.

Andreas Albrecht, Defect models of cosmic structure in light of the new CMB data, XXXVth Rencontres de Moriond ``Energy Densities in the Universe" (2000).

Fitting CMB data with cosmic strings and inflation, by Neil Bevis, Mark Hindmarsh, Martin Kunz, and Jon Urrestilla 2008 PRL100.021301

The inflationary paradigm is successful in providing a match to measurements of the cosmic microwave background (CMB) radiation, and it appears that **any successful theory of high energy physics must be able to incorporate inflation**. While ad hoc single-field inflation can provide a match to the data, **more theoretically motivated models commonly predict the existence of cosmic strings**. These strings are prevalent in supersymmetricinflation models and occur frequently in grand-unified theories (GUTs). String theory can also yield strings of cosmic extent. Hence the observational consequences of cosmic strings are important, including their sourcing of additional anisotropies in the CMB radiation. In this letter we present a multi-parameter fit to CMB data for models incorporating cosmic strings. It is the first such analysis to use simulations of a fully dynamical network of local cosmic strings, and the first to incorporate their microphysics with a field theory. It yields conclusions which differ in significant detail from previous analyses based upon simplified models: **we find that the CMB data moderately favor a 10% contribution from strings to the temperature power spectrum** measured at multipole $\ell = 10$ with a corresponding spectral index of primordial scalar perturbations $n_s \simeq 1$. There are also important implications for models of inflation with blue power spectra ($n_s > 1$). These are disfavored by CMB data under the concordance model (power-law CDM which gives $n_s = 0.951+0.015 -0.019$) and previous work seemed to show that this remains largely the case even if cosmic strings are allowed. However with our more complete CMB calculations, we find that the CMB puts no pressure on such models if they produce cosmic strings. Our conclusions are slightly modified when additional non-CMB data are included, with the preference for strings then reduced.

GUT Monopoles

A simple SO(3) GUT illustrates how nonsingular monopoles arise. The Lagragian is

$$\begin{aligned}
\mathcal{L} &= \frac{1}{2}D_\mu\Phi^a D^\mu\Phi^a - \frac{1}{4}F^a_{\mu\nu}F^{a\mu\nu} - \frac{1}{8}\lambda(\Phi^a\Phi^a - \sigma^2)^2, \\
F^a_{\mu\nu} &= \partial_\mu A^a_\nu - \partial_\nu A^a_\mu - e\varepsilon_{abc}A^b_\mu A^c_\nu, \\
D_\mu\Phi^a &= \partial_\mu\Phi^a - e\varepsilon_{abc}A^b_\mu\Phi^c.
\end{aligned}$$

The masses of the resulting charged vector and Higgs bosons after spontaneous symmetry breaking are

$$\begin{aligned}
M_V^2 &= e^2\sigma^2, \\
M_S^2 &= \lambda\sigma^2.
\end{aligned}$$

If the Higgs field Φ^a happens to rotate about a sphere in SO(3) space as one moves around a sphere about any particular point in $\mathbf{x}$-space, then it must vanish at the particular point. Remarkably, if we identify the massless vector field as the photon, this configuration corresponds to a nonsingular magnetic monopole, as was independently discovered by 'tHooft and Polyakov. The monopole has magnetic charge twice the minimum Dirac value, $g = 2\pi/e = (4\pi/e^2)(e/2) \approx 67.5\ e$.

The singular magnetic field is cut off at scale σ, and as a result the GUT monopole has mass $M_{monopole} \approx M_V/\alpha \approx M_{GUT}/\alpha \approx 10^{18}$ GeV.

GUT Monopole Problem

The Kibble mechanism produces ~ one GUT monopole per horizon volume when the GUT phase transition occurs. These GUT monopoles have a number density over entropy

$$n_M/s \sim 10^2 (T_{GUT}/M_{Pl})^3 \sim 10^{-13}$$

(compared to $n_B/s \sim 10^{-9}$ for baryons) Their annihilation is inefficient since they are so massive, and as a result they are about as abundant as gold atoms but 10^{16} times more massive, so they "overclose" the universe. This catastrophe must be avoided! **This was Alan Guth's initial motivation for inventing cosmic inflation.**